

---

# Sharp feature-learning transitions and Bayes-optimal neural scaling laws in extensive-width networks

---

Minh-Toan Nguyen  
ICTP  
Trieste, Italy  
mnguyen@ictp.it

Jean Barbier  
ICTP  
Trieste, Italy  
jbarbier@ictp.it

## Abstract

We study the information-theoretic limits of learning a one-hidden-layer teacher network with hierarchical features from noisy queries, in the context of knowledge transfer to a smaller student model. We work in the high-dimensional regime where the teacher width  $k$  scales linearly with the input dimension  $d$  – a setting that captures large-but-finite-width networks and has only recently become analytically tractable. Using a heuristic leave-one-out decoupling argument, validated numerically throughout, we derive asymptotically sharp characterizations of the Bayes-optimal generalization error and individual feature overlaps via a system of closed fixed-point equations. These equations reveal that feature learnability is governed by a sequence of sharp phase transitions: as data grows, teacher features become recoverable sequentially, each through a discontinuous jump in overlap. This sequential acquisition underlies a precise notion of *effective width*  $k_c$  – the number of learnable features at a given data budget  $n$  – which unifies two distinct scaling regimes: a feature-learning regime in which the Bayes-optimal generalization error  $\varepsilon^{\text{BO}}$  scales as  $n^{1/(2\beta)-1}$ , and a refinement regime in which it scales as  $n^{-1}$ , where  $\beta > 1/2$  is the exponent of the power-law feature hierarchy. Both laws collapse to the single relation  $\varepsilon^{\text{BO}} = \Theta(k_c d/n)$ . We further show empirically that a student trained with ADAM near the effective width  $k_c$  achieves these optimal scaling laws (up to a small algorithmic gap), and provide an information-theoretic account of the associated scaling in model size.

## 1 Introduction

The performance of large neural networks often follows simple power laws in data, compute, and model size [26, 31, 28]. A growing line of theory attributes this regularity to a hierarchical organization of the target function: features carry geometrically decaying importance and a learner acquires them roughly in order [29, 34, 2, 36, 22, 20]. In a teacher-student setting – the basic primitive behind data-driven model distillation [11, 27, 25] – this hierarchy raises an immediate design question: at a fixed data budget, how should one size the student?

Figure 1 exhibits two empirical regularities for an ADAM-trained student. (i) There is a critical width beyond which the test error *increases* (middle panel); below this threshold, the error follows a power law in model size with exponent  $1 - 2\beta$  for a power-law feature hierarchy of exponent  $\beta > 1/2$ . (ii) At or near the optimal width, the error obeys two distinct power laws in  $n$  (right panel): a slow regime with exponent  $1/(2\beta) - 1$  and a faster regime with exponent  $-1$ . These are striking but mechanism-agnostic: they could reflect properties of ADAM, or fundamental information-theoretic constraints. To disentangle the two, we lift all computational constraints and adopt a Bayes-optimal viewpoint, asking:

**Q1.** *Given a fixed dataset, which features of the teacher are statistically recoverable?*

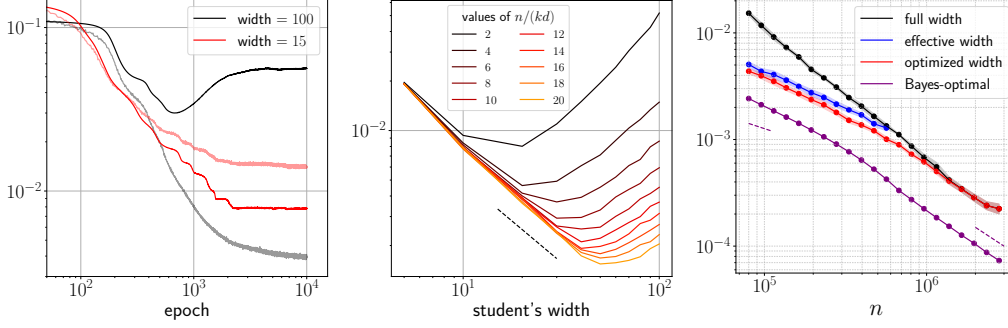


Figure 1: ADAM-trained students (all curves except the purple one, right panel) on a teacher with  $\sigma(x) = \tanh(2x)$  (with the  $2x$  matching the convention in [6]),  $k = 100$ ,  $d = 200$ ,  $\Delta = 0.01$ , power-law readout with  $\beta = 1$  (3 batches,  $10^4$  epochs, learning rate 0.003; averages over 9 runs, shaded regions show  $\pm 1$  standard deviation). **Left:** At fixed sample rate  $n/(kd) = 2$ , a reduced-width student (solid = test error; faint = training error) outperforms the full-width one. **Middle:** Generalization error vs. student width  $k_s$  at several sample rates  $n/(kd)$ . Performance degrades beyond a critical width; the dashed line indicates the theoretically predicted optimal model-size exponent  $1 - 2\beta$ . **Right:** Generalization error vs. data size  $n$  for three width choices – *full-width* ( $k_s = k$ ), *effective width* ( $k_s = k_c$  from theory), and *optimized width* (best-performing  $k_s \in \{10, 20, \dots, 100\}$  found by grid search) – together with the Bayes-optimal prediction (purple). Dashed lines indicate the predicted scaling exponents:  $1/(2\beta) - 1$  in the *feature-learning regime* and  $-1$  in the *refinement regime*, see Section 3 and Appendix G for the derivation of exponents.

**Q2.** How does the recoverable subset of features constrain the scaling law of the Bayes-optimal generalization error  $\varepsilon^{\text{BO}}$  in the data size  $n$ ?

We address **Q1** and **Q2** in a one-hidden-layer teacher–student model in the *extensive-width* regime  $k = \Theta(d)$ , with  $k$  the teacher width and  $d$  the input dimension. This regime captures the large-but-finite width of practical networks, lies strictly between the well-studied multi-index ( $k = \Theta(1)$ ) and NTK ( $k \gg d$ ) extremes, and is the minimal setting for non-trivial feature learning beyond the linear data scale ( $n \gg d$ ). Our analytical handle is a heuristic leave-one-out (cavity) decoupling argument, validated numerically throughout.

**Paper organization.** Section 1.1 introduces the model and hypotheses. The main results – fixed-point equations for the feature overlaps and Bayes-optimal error, and the ensuing scaling laws – are stated in Section 2 and analyzed in Section 3, which covers the phase transitions, the error decomposition, the two scaling regimes and their unification via  $k_c$ , and the ADAM-trained student. The leave-one-out derivation is in Section 4. Section 5 concludes. Derivations, numerical methods, and additional asymptotic results are collected in the Appendices. The code for the simulations in this paper is publicly available at <https://github.com/Minh-Toan/scaling-laws>.

## 1.1 Problem setup

**Notations.** In addition to the standard  $O$ -notation, we write  $A \simeq B$  if  $A - B = o(1)$ ;  $A \sim B$  if  $A/B \simeq 1$ , and with a slight abuse of notation, we also use  $\sim$  to indicate a random variable following a probability law;  $A \gtrsim B$  means  $A \geq cB$  for some absolute constant  $c > 0$ ;  $A = \Theta(B)$  if  $cB \leq A \leq CB$  for absolute  $c, C > 0$ ;  $A = \Theta_p(B)$  if  $c, C$  may depend on parameter  $p$ .

**Teacher and dataset.** Given inputs  $\mathbf{x}_\mu$  drawn i.i.d. from  $\mathcal{N}(0, \mathbf{I}_d)$  and noise variables  $z_\mu$  that are i.i.d. standard Gaussian, the dataset  $\mathcal{D} = (\mathbf{x}_\mu, y_\mu^{\text{out}})_{\mu \in [n]}$  consists of input-output pairs with noisy responses  $y_\mu^{\text{out}} = y_\mu + \sqrt{\Delta} z_\mu$  and clean responses generated by the teacher neural network:

$$y_\mu = \mathbf{v}^\top \sigma(\mathbf{W}^0 \mathbf{x}_\mu). \quad (1)$$

$\sigma$  is an element-wise activation,  $\mathbf{v} \in \mathbb{R}^k$  is the readout vector, and  $\mathbf{W}^0 \in \mathbb{R}^{k \times d}$  is the teacher’s weight matrix. Each row  $\mathbf{w}_i^0$  of  $\mathbf{W}^0$  defines a latent direction – a *feature* – used to project the input.

**Students.** We study two types of learners. The *Bayesian student* knows the data-generation mechanism (activation  $\sigma$ , prior  $P_0$ , noise variance  $\Delta$ , and readout  $\mathbf{v}^1$ ) but not the specific realization  $\mathbf{W}^0$ . For a new input  $\mathbf{x}$ , it predicts the corresponding teacher’s output by computing the posterior mean  $\mathbb{E}[\mathbf{v}^\top \sigma(\mathbf{W}\mathbf{x}) \mid \mathcal{D}]$ , which achieves the minimum mean square error, also known as the *Bayes-optimal error*  $\varepsilon^{\text{BO}}$ . On the other hand, the *SGD student* is a one-hidden-layer network of width  $k_s \leq k$  and same input dimension  $d$ , with weights  $(\mathbf{W}, \mathbf{v})$  trained with ADAM. The  $L_2$  norm of each  $\mathbf{w}_i$  is normalized after every epoch to prevent excessive weight growth and improve performance.

We work throughout under the following hypotheses.

(H1) *High-dimensional extensive-width regime.* We work in the scaling regime

$$d \gg 1, \quad k = \Theta(d), \quad n \gg d. \quad (2)$$

The condition  $k = \Theta(d)$  sits strictly between the multi-index regime ( $k = \Theta(1)$ ), where expressivity is limited, and the NTK regime ( $k \gg d$ ), where the model is lazy [30, 14, 24]. It is the minimal setting for non-trivial feature learning at the super-linear data scale. The condition  $n \gg d$  is necessary to move beyond the linear-model regime  $n = \Theta(d)$  [15, 13].

(H2) *Hierarchical readouts.* We assume  $\|\mathbf{v}\|^2 = 1$  and  $v_1 \geq v_2 \geq \dots \geq v_k \geq 0$ , so  $v_i$  controls the signal-to-noise ratio for feature  $i$ : features with larger  $v_i$  are easier to recover. We consider readouts that are *dense* ( $\sqrt{k} \mathbf{v}$  has a limiting density); *power-law* ( $v_i \propto i^{-\beta}$ ); *exponential* ( $v_i \propto e^{-ci}$ ); and *ultra-sparse* (all but  $\Theta(1)$  entries vanish). To derive scaling laws we focus on  $\beta > 1/2$ .

(H3) *Teacher weights.*  $\mathbf{W}^0$  is drawn uniformly from the Stiefel manifold of  $k \times d$  matrices with orthonormal rows ( $k \leq d$ ). The BO error is asymptotically unchanged under i.i.d. Gaussian  $\mathbf{W}^0$ ; the orthonormal ensemble reduces fluctuations and yields cleaner numerical results.

(H4) *Activation.*  $\sigma$  is differentiable, and  $\sigma, \sigma'$  are square-integrable w.r.t.  $\mathcal{N}(0, 1)$ . Moreover,  $\sigma$  satisfies  $\mu_2 := \mathbb{E}_{z \sim \mathcal{N}(0,1)}[\sigma(z)(z^2 - 1)] = 0$ , i.e. the second Hermite coefficient vanishes (Appendix A). This holds for odd activations and is a condition needed for the “neuron decoupling” central to our leave-one-out analysis (as in [36]). The complementary regime  $\mu_2 \neq 0$  is studied in [33].

## 1.2 Contributions

**Sharp staircase of feature-learning transitions (answers Q1; Result 1.1).** We derive a closed system of fixed-point equations for the individual feature overlaps  $(q_i)_{i=1}^k$  and the Bayes-optimal error  $\varepsilon^{\text{BO}}$ , valid for arbitrary readout distributions. Feature  $i$  is recoverable ( $q_i > 0$ ) if and only if its self-consistent SNR  $\text{snr}_i = (n/d) v_i^2 / (\Delta + \varepsilon^{\text{BO}})$  exceeds an activation-dependent threshold  $\lambda_\sigma$ . The  $(q_i)$  cross it sequentially as  $n$  grows, producing a staircase of discontinuous overlap jumps and matching drops in  $\varepsilon^{\text{BO}}$  (Fig. 2) – this mirrors what happens dynamically under SGD training [36]. The number  $k_c \leq k$  of features above threshold defines the *effective width* of the teacher, i.e. the number of information-theoretically learnable features given a fixed data budget.

**Bayes-optimal scaling laws unified through  $k_c$  (answers Q2; Result 1.2–3).** The Bayes-optimal error decomposes transparently as  $\varepsilon^{\text{BO}} = \Theta(k_c d/n) + \Theta(\sum_{j>k_c} v_j^2)$ , i.e. a finite-sample term contributing  $\Theta(d/n)$  per learnable feature plus an irreducible bias from the unlearned ones. For power-law readouts with  $\beta > 1/2$  the second term is dominated by the first, collapsing both regimes of Fig. 1 (right) to the single relation  $\varepsilon^{\text{BO}} = \Theta(k_c d/n)$ . The two empirical regimes then arise from the two asymptotics of  $k_c(n)$ :  $k_c \sim (n/d)^{1/(2\beta)}$  in the *feature-learning* regime ( $n \ll k^{2\beta} d$ ), giving  $\varepsilon^{\text{BO}} \sim n^{1/(2\beta)-1}$ , and  $k_c = k$  in the *refinement* regime ( $n \gg k^{2\beta} d$ ), recovering the classical parametric rate  $n^{-1}$ . The same picture explains the model-size behavior of the ADAM-trained student in Fig. 1: a width- $k_s$  student near  $k_c$  matches the Bayes-optimal data-size exponents, while wider students overfit non-learnable directions (up to a small residual gap at the weakest features that we attribute to a computational–statistical threshold, see Section 3).

**A leave-one-out approach beyond dense readouts.** Methodologically, our cavity argument reduces multi-feature inference to a sequence of independent scalar generalized linear models, without recourse to the replica method and for arbitrary readout structures. As a special case it recovers the dense-readout result of [6] (originally obtained via replicas) and extends it: we characterize the full

<sup>1</sup>Assuming  $\mathbf{v}$  is known to the Bayesian student is a convenient simplification. However, in the scaling regime we consider,  $k = \Theta(d)$ , it does not change the Bayes-optimal (BO) error compared to the case where  $\mathbf{v}$  is unknown as proved in [6].

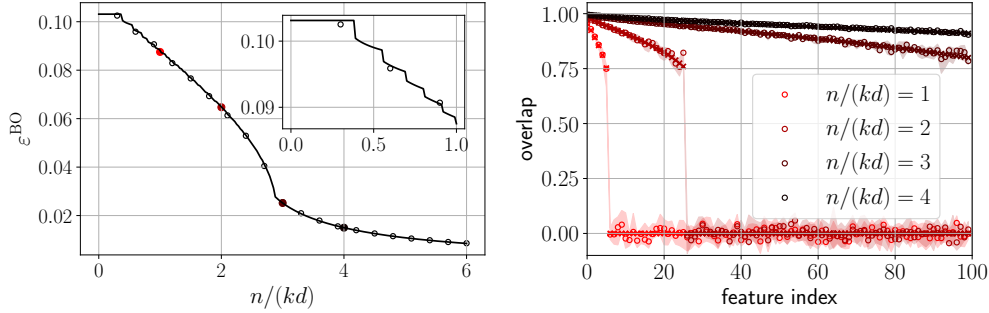


Figure 2: Bayes-optimal learning curve (**left**) and feature overlaps at selected values of  $n/(kd)$  (**right**) for  $\sigma(x) = \tanh(2x)$ ,  $d = 200$ ,  $k = 100$ ,  $\Delta = 0.04$ , power-law readout with  $\beta = 0.3$ . Solid lines and crosses: theoretical predictions from the fixed-point equations (6); circles: averages over 9 independent Hamiltonian Monte Carlo experiments; shaded regions:  $\pm 1$  standard deviation. Markers on the learning curve indicate the  $n/(kd)$  values at which the overlap profiles on the right are evaluated. The inset shows the staircase of discontinuous drops in  $\epsilon^{\text{BO}}$  as successive features are learned (see §1.2). For  $\beta < 1/2$ , the error decay upon entering the refinement regime is slower than  $n^{-1}$ ; see Section 3 for the comparison with the  $\beta > 1/2$  case.

decay rate of  $\epsilon^{\text{BO}}$  as a function of readout sparsity, where the dense case only yields  $\Theta(1)$ , while it can quickly decrease with  $d$  for sparser readouts. The analysis covers all activations with vanishing second Hermite coefficient ( $\mu_2 = 0$ ), in particular all odd activations, complementing the  $\mu_2 \neq 0$  regime treated in [20, 33].

### 1.3 Additional related works

**Multi-index models.** Multi-index models (teacher width  $k = \Theta(1)$  in the context of neural networks) are a well-developed testbed for feature learning in SGD [3, 1, 18], Bayes-optimal [7, 4, 38], and computationally-hard [16, 17] regimes. Despite these important insights, multi-index models remain weakly expressive, and a recent substantial technical effort has been devoted to going beyond this fixed-width setting [15, 13, 33, 36, 22, 6]. The present work contributes to this research line.

**Neural scaling laws.** Neural scaling laws have been studied from two broad perspectives. A first line of work operates in the non-feature-learning regime – kernel methods, random feature models, or linear regression – and derives scaling laws from spectral assumptions on the data covariance. Several of these works obtain scaling laws in both data size and model size [5, 10, 32], or characterize how the optimal model size scales with compute budget [35]. A second line of work introduces genuine feature learning, either through abstract task models [29, 34, 23, 12] or through concrete neural network models in the multi-index or sublinear-width regime [2, 36, 22, 20]. The quantization model of [34] is phenomenologically close to our framework: it postulates that networks learn discrete units of knowledge sequentially, in order of their contribution to loss, and that model capacity caps the number of learnable units. These properties instead emerge from first principles in our model.

Our closest predecessor [20] derives data-size scaling laws in the multi-index regime  $k = \Theta(1)$  (numerically:  $k = 10$ ,  $d = 1000$ , vs.  $k = 100$ ,  $d = 200$  here), using a hand-crafted rather than standard generalization error, and restricted to activations with  $\mu_2 \neq 0$ ; ours are complementary, covering  $\mu_2 = 0$  and hence all odd activations. On the algorithmic side, the optimal scaling laws in [20] are achieved by AMP, later extended in [19] to activations with  $\mu_2 \neq 0$  and even to even functions with  $\mu_2 = 0$ : for AMP, the data-limited exponent acquires a multiplicative correction from a noise-sensitive exponent defined therein, while the information-theoretic exponents are conjectured to be unchanged. Despite all these differences, these three works obtain the same BO data-size scaling exponent, suggesting universality across activation classes and width regimes.

**Bayes-optimal learning of extensive-width networks.** In the linear data regime  $n = \Theta(d)$ , the BO problem reduces to linear regression [15, 13]. For quadratic activations at  $n = \Theta(d^2)$ , [33] characterized the BO error but found no feature recovery, due to rotational symmetry intrinsic to this specific setting. The general case was resolved by [6] using the replica method from physics, for dense readouts and multiple layers. Our work specializes to one hidden layer and  $\mu_2 = 0$ , but generalizes to

arbitrary readout structure. Moreover, the present leave-one-out approach, though remaining heuristic, is arguably more direct and does not require familiarity with the replica formalism.

## 2 Main results

Before stating the results, we introduce the following definitions. For an input  $\mathbf{x}$ , we denote the corresponding response by  $y(\mathbf{x}, \mathbf{W}^0) := \mathbf{v}^\top \sigma(\mathbf{W}^0 \mathbf{x})$ , which emphasizes the dependence of the label on  $\mathbf{W}^0$  (the readout  $\mathbf{v}$  being fixed). Given a response predictor  $\hat{y}(\mathbf{x}, \mathcal{D})$ , we use the standard definition of mean square (prediction) error (MSE):  $\mathbb{E}_{\mathcal{D}, \mathbf{W}^0} \mathbb{E}_{\mathbf{x} \sim \mathcal{N}(0, \mathbf{I}_d)} (y(\mathbf{x}, \mathbf{W}^0) - \hat{y}(\mathbf{x}, \mathcal{D}))^2$ . Recall that the Bayes-optimal error  $\varepsilon^{\text{BO}}$  is attained by the Bayesian student  $\hat{y}(\mathbf{x}, \mathcal{D}) = \mathbb{E}[y(\mathbf{x}, \mathbf{W}) \mid \mathcal{D}] =: \langle y(\mathbf{x}, \mathbf{W}) \rangle$ , where the bracket notation  $\langle \cdot \rangle$  is used to denote an average w.r.t. the Bayesian posterior distribution:  $\mathbf{W} \sim P(\mathbf{W} \mid \mathcal{D}) \propto \nu(\mathbf{W}) \prod_{\mu \leq n} \exp(-\frac{1}{2\Delta} (y_\mu^{\text{out}} - y(\mathbf{x}_\mu, \mathbf{W}))^2)$ , with  $\nu(\cdot)$  the uniform measure over the Stiefel manifold of  $k \times d$  matrices with orthonormal rows.

For any function  $\sigma \in L_g^2$ , define the kernel  $g_\sigma$  on  $[0, 1]$  and  $m_\sigma$  on  $[0, \infty)$  as

$$g_\sigma(x) := \mathbb{E}[\sigma(z_1)\sigma(z_2)], \quad (z_1, z_2) \sim \mathcal{N}\left(0, \begin{bmatrix} 1 & x \\ x & 1 \end{bmatrix}\right), \quad (3)$$

$$m_\sigma(\lambda) := \arg \max_{q \in [0, 1]} \{\lambda g_\sigma(q) + q + \ln(1 - q)\}. \quad (4)$$

We also define  $\lambda_\sigma := \sup\{\lambda \geq 0 : m_\sigma(\lambda) = 0\}$ . Basic properties of the functions  $g_\sigma$  and  $m_\sigma$  are established in Appendix D. We will see in Section 4 that  $m_\sigma(\lambda)$  is related to the overlap between signal and Bayes estimator of a single feature/latent direction in the context of a generalized linear model in a ‘‘high sample rate’’ regime [7], see Result 3. It is non-decreasing with a discontinuity at  $\lambda_\sigma$  (Appendix D).  $\lambda_\sigma$  is thus the critical SNR below which no estimator can recover the feature.

**A note on rigor.** The extensive-width regime  $k = \Theta(d)$  of Bayesian neural networks is particularly challenging to analyze, with only few rigorous results in simpler settings, see e.g. [13]. Our derivations are therefore non-rigorous, but based on powerful heuristic approaches: the cavity (leave-one-out) method and on hypothesized Gaussianity of so-called cavity fields – techniques standard in statistical physics that are proved rigorously in simpler related models [37, 7, 9] and conjectured to extend here. They rely on concentration properties of the posterior; in particular,

$$\mathbb{E} \langle (\mathbf{w}_i^0 \cdot \mathbf{w}_j^1)^2 \rangle = O(d^{-1}) \text{ for } i \neq j, \quad \mathbb{E} \langle (\mathbf{w}_i^0 \cdot \mathbf{w}_i^1 - q_i)^2 \rangle = O(d^{-1}), \quad (5)$$

for  $\mathbf{W}^1 \sim P(\cdot \mid \mathcal{D})$ . In words, we assume that distinct features decouple under the posterior, and that each overlap concentrates to a deterministic limit  $q_i$ . The feature-decoupling assumption is proved in Appendix F for the special case of dense readouts in the extensive-width, near-interpolation regime discussed in Section 3, while the proof of the overlap concentration between matched features  $\mathbf{w}_i^0 \cdot \mathbf{w}_i^1$  follows from a direct application of standard perturbation techniques from mathematical physics [8]. We assume that these concentrations continue to hold in the more general scaling regimes considered in the paper without proof. All predictions are vindicated by Hamiltonian Monte Carlo simulations across all parameter regimes, with excellent agreement already at  $d \sim 10^2$ .

Before stating the results, let us mention that if one removes the linear component of the activation  $\sigma$ , i.e. replace it by  $\tilde{\sigma}(x) := \sigma(x) - \mu_0 - \mu_1 x$ , then the overlaps  $q_i$  and Bayes-optimal error we derive remain asymptotically the same (Appendix C). Consequently, in the subsequent claims, we assume without loss of generality that  $\mu_0 = \mu_1 = 0$  in addition to our assumption  $\mu_2 = 0$ ; in other words,  $\sigma$  has *information exponent* at least 3 [3], as in the complementary dynamical analysis of [36].

**Result 1.** *Consider the setting described in Section 1.1. For  $i \in \mathbb{N}$ , let  $\mu_i$  be the  $i$ -th Hermite coefficient of  $\sigma$  (Appendix A).*

1. **Feature overlaps and Bayes-optimal error:** *Overlaps  $(q_i)_{i=1}^k$  solve the fixed-point system*

$$q_i = m_\sigma\left(\frac{nv_i^2/d}{\Delta + \varepsilon}\right), \quad \varepsilon = \sum_{i=1}^k v_i^2 (g_\sigma(1) - g_\sigma(q_i)) \quad (6)$$

*and the BO error satisfies  $\varepsilon^{\text{BO}} \sim \varepsilon$ . Feature  $i \in [k]$  is learnable if  $q_i > 0$ . Denote by  $k_c = k_c(k, d, n) = |\{i : q_i > 0\}|$  the effective width of the teacher.*

2. **Asymptotic decomposition of the BO error.** The optimal error decomposes as

$$\varepsilon^{\text{BO}} = \Theta\left(\frac{k_c d}{n}\right) + \Theta\left(\sum_{j>k_c} v_j^2\right). \quad (7)$$

The first term corresponds to the estimation error on learnable features; the second to the irreducible error from non-learnable features.

3. **Bayes-optimal scaling law.** Fix  $k, d$  for the teacher (and for the Bayes-optimal student). Consider power-law distributed readouts with exponent  $\beta > 1/2$ . From eq. (7) and the characterization of  $k_c$  in Appendix G, the Bayes-optimal error and effective width obey the following scalings:

$$\varepsilon^{\text{BO}} = \begin{cases} \Theta_{k,d}(n^{\frac{1}{2\beta}-1}) \\ \Theta_{k,d}(n^{-1}) \end{cases} \quad k_c = \begin{cases} \Theta_{k,d}(n^{1/(2\beta)}) & n \ll k^{2\beta} d \\ k & n \gg k^{2\beta} d \end{cases} \quad \begin{array}{l} \text{(feature-learning regime),} \\ \text{(refinement regime).} \end{array}$$

The numerical method used to solve (6) is described in Appendix K.1. This procedure consistently finds a single solution. Uniqueness can be easily checked numerically via the one-parameter equation (60) over  $\varepsilon$ . Uniqueness for  $\varepsilon$  then implies the one for the  $(q_i)$  via (6).

*Remark 2* (Statistical compressibility). When  $k_c < k$  the teacher is *compressible*. The same leave-one-out Gaussian argument (Section 4) suggests that the  $n$  teacher responses are statistically indistinguishable – in the sense of equal Bayes-optimal error – from those of the reduced model

$$y_\mu = \mathbf{v}_{1:k_c}^\top \sigma(\mathbf{W}_{1:k_c}^0 \mathbf{x}_\mu) + \sqrt{\Delta + \Delta'} z_\mu, \quad \Delta' := g_\sigma(1) \sum_{j>k_c} v_j^2. \quad (8)$$

Indeed, by definition of  $k_c$ , the terms  $\sum_{i>k_c} v_i \sigma(\mathbf{w}_i^0 \cdot \mathbf{x}_\mu)$  are not learnable and act as effective noise with variance  $\Delta'$ . When  $k - k_c \gg 1$ , a central limit/Gaussianity assumption applied to this noise and combined with the label noise yields the reduced model (8). This is the information-theoretic basis for the empirical finding that a reduced-width student can outperform a full-width one (Fig. 1, left). On the other hand, when  $k - k_c = O(1)$ , the Gaussian approximation does not hold for the noise induced by the non-learnable terms. However, this contribution is negligible compared to  $\Delta$ .

### 3 Discussion

**Sharp staircase learning transitions.** Consider the system (6). Since  $m_\sigma(x) = 0$  if  $x \leq \lambda_\sigma$  by definition, the feature  $i$  is learnable if and only if

$$\text{snr}_i := \frac{(n/d)v_i^2}{\Delta + \varepsilon} > \lambda_\sigma. \quad (9)$$

The *effective signal-to-noise ratio*  $\text{snr}_i$  entering (6) is determined by the  $i$ -th feature strength  $v_i^2$  (which depends on  $k$ , e.g. it scales as  $1/k$  in the dense case), the sampling rate  $n/d$ , and the effective noise variance  $\Delta + \varepsilon$ . As  $n$  grows, and assuming that  $v_{i+1} > v_i$  strictly,  $(\text{snr}_i)_i$  grow and cross the threshold (9) sequentially – thus increasing  $k_c$  –, leading to a staircase sequence of phase transitions, see Fig. 2 (left panel) and [36, 20] for similar phenomena in settings of sub-linear width ( $k \ll d$ ).

**Decomposition of the Bayes-optimal error.** Equation (7) has a transparent interpretation. Firstly, the underlying mechanism is that each learned feature contributes  $\Theta(d/n)$  to the generalization error, while a non-learned feature  $i$  contributes  $\Theta(v_i^2)$ . Secondly, writing  $\varepsilon^{\text{BO}} = \Theta(k_c d/n)$  when the second term is negligible, the BO error scales as the inverse of the *effective sampling rate*  $n/(k_c d)$ : the teacher behaves as a model with  $k_c$  features, each requiring  $\Theta(d)$  samples to estimate. The data-size scaling laws of  $\varepsilon^{\text{BO}}$  in both regimes thus follow directly from how  $k_c$  depends on  $n$  (Fig. 1).

**Bayes-optimal scaling law.** With power-law readouts with  $\beta > 1/2$ , the crossover at  $n^* = \Theta(k^{2\beta} d)$  in the scaling law for  $\varepsilon^{\text{BO}}$  marks the point at which the weakest feature  $k$  becomes learnable. i.e. the smallest  $n$  s.t.  $(n/d)v_k^2 = \Theta((n/d)k^{-2\beta}) \gtrsim \lambda_\sigma$ . For  $n \ll n^*$ , only  $k_c = \Theta((n/d)^{1/(2\beta)}) \ll k$  features are above threshold and are learned sequentially; with  $k_c$  defined by the condition that  $\text{snr}_{k_c} \propto (n/d)k_c^{-2\beta}$  is greater than the threshold  $\lambda_\sigma$  while  $\text{snr}_{k_c+1}$  is not, see Appendix G for more details. Instead, when  $n \gg n^*$  all features are learned (i.e. have overlap  $q_i > 0$ ) and additional data only refines them, yielding the feature-learning vs. refinement regimes, see Fig. 1.

Still with  $\beta > 1/2$ , the second error term in (7) corresponding to non-learnable features is of order smaller or equal to the error corresponding to learnable feature, see Appendix G. Consequently, both scaling laws unify into the single expression involving the effective sampling rate  $n/(k_c d)$ :

$$\varepsilon^{\text{BO}} = \Theta(k_c d/n). \quad (10)$$

In the feature-learning regime  $k_c$  grows with  $n$ , which partially offsets the  $1/n$  decay and yields the slower exponent  $1/(2\beta) - 1 < 1$ ; in the refinement regime  $k_c = k$  is fixed, recovering the  $n^{-1}$  rate. The effective width  $k_c$  thus provides a unified account of both scaling regimes. These scaling laws provide a concrete theoretical instantiation of the quantization model of [34]: their *capacity hypothesis* – that the number of learnable quanta grows with model size – emerges here directly from the width bottleneck below  $k_c$  and the sharp SNR threshold  $\lambda_\sigma$ .

We emphasize that the analytic formula  $k_c = \Theta((n/d)^{1/(2\beta)})$  in the feature-learning regime provides a first-principles prescription for the optimal student width directly from the data budget, without retraining at each candidate model size – a concrete theoretical underpinning for *hyperparameter transfer* of model width [39]: rather than fitting the optimal size empirically by training multiple students, the exponent  $\beta$  of the feature hierarchy determines how to optimally scale the model width  $k_s$  as  $n$  varies, in the same spirit as compute-optimal scaling laws [28].

As a final remark, although the scaling within the refinement regime is  $n^{-1}$  in both cases, the behavior of the BO error just before entering this regime differs between  $\beta > 1/2$  and  $\beta < 1/2$ . When  $\beta < 1/2$  and  $i \sim k$ , we have  $v_i^2 \sim (1 - 2\beta)i^{-2\beta}k^{2\beta-1} \sim (1 - 2\beta)k^{-1}$ , meaning that near the edge  $\mathbf{v}$  behaves like a dense vector. Consider the two cases close to entering the refinement regime: for the same fractional increase in the data size, since many features become learnable when  $\beta < 1/2$  due its dense-like behavior, it yields a steeper descent before the refinement regime is reached (Fig. 2).

**Scaling laws for SGD-trained student.** We now discuss the empirical findings of Fig. 1 for SGD-trained students under the same fixed-teacher setting as before with power-law readout of exponent  $\beta > 1/2$ , namely that there exist: (1) a critical (i.e., optimized) width beyond which performance under ADAM degrades, with a scaling law in model size that holds up to this threshold, and (2) two distinct scaling laws in data size, corresponding again to feature learning and refinement regimes.

*Scaling with model size.* We start by discussing the scaling with model size when the student width  $k_s$  lies below the critical width, which is itself smaller than  $k$ . In this case, the number of features that the student can learn is equal to its width  $k_s$ . This is related to the *capacity hypothesis* in [34].

On the other hand, we observe empirically a mechanism similar to that underlying (7): each learned feature contributes  $\Theta(d/n)$  to the generalization error, while each non-learned feature  $i$  contributes a term of order  $\Theta(v_i^2)$ . Accordingly, the errors contributed by learned and non-learned features are  $\Theta(k_s d/n)$  and  $\Theta(\sum_{j>k_s} v_j^2)$  respectively. Since the student cannot learn more features than the BO student, we have  $k_c \geq k_s$ , leading to

$$\sum_{j>k_s} v_j^2 \geq \sum_{j>k_c} v_j^2 \gtrsim k_c d/n \geq k_s d/n$$

where the second inequality holds in the feature-learning regime (Appendix G), i.e. the current setting. Thus the SGD-student’s error is  $\Theta(\sum_{i>k_s} v_i^2) = \Theta(\sum_{i>k_s} i^{-2\beta}) = \Theta(\int_{k_s}^k x^{-2\beta} dx) = \Theta(k_s^{1-2\beta})$ , giving the power-law scaling in model size with exponent  $1 - 2\beta$  (dashed line, Fig. 1, middle).

Note that the optimally-sized student has a lower error overall, but a flatter slope in  $n$ , than the full-width student in the feature-learning regime: precisely because it avoids fitting non-learnable directions, it starts from a lower error floor and gains less from each additional sample.

*Scaling with data.* That the exponents for the error as a function of  $n$  of the SGD-trained model match the Bayes-optimal ones in the two regimes (Fig. 1, right panel) can be argued as follow. Firstly, a student of width  $k_s \gg k_c$  overfits non-learnable directions; one near  $k_c$  avoids this, as confirmed by Fig. 1 (right). We conjecture that in this non-overfitting regime, ADAM learnability mirrors the Bayes-optimal one: feature  $i$  is recoverable if and only if  $(n/d)v_i^2$  exceeds an algorithmic threshold  $\lambda_\sigma^{\text{algo}} \geq \lambda_\sigma$ , with the inequality reflecting a possible computational-to-statistical gap [6] which can be present for ADAM, see [6]. Under this conjecture, the scaling-law derivation above applies verbatim, yielding the same exponents. This conjecture is supported by numerics, and is provably correct in simpler models, in particular in the generalized linear model – which is closely connected to

the present model via the leave-one-out argument in the next section – when using the Bayesian approximate message-passing algorithm [9, 7].

We note one deviation from the predicted  $n^{-1}$  slope at large  $n$  in the refinement regime: roughly 5% of the weakest features remain non-learnable under ADAM, causing the empirical exponent to deteriorate. This residual gap in Fig. 1 (right) points to a small but persistent computational-to-statistical gap for the weakest features, and is consistent with an algorithmic threshold  $\lambda_\sigma^{\text{algo}} > \lambda_\sigma$ .

**Extensive-width, near-interpolation regime.** We also analyzed the linear-width, near-interpolation regime scaling regime  $k \sim \gamma d$ ,  $n \sim \alpha d^2$  ( $\alpha, \gamma > 0$  fixed), where  $k$ ,  $d$ , and  $n$  diverge *together* – a regime with rich feature-learning phenomenology that attracts strong theoretical interest [33, 6, 13, 21] connected to compute-optimal scaling in large language models [28]. The table below (Appendix H) reports the asymptotic  $\varepsilon^{\text{BO}}$  and effective width  $k_c$  for readout distributions of increasing sparsity in this regime. The  $\Theta(\cdot)$  rates are in  $d$  as  $d \rightarrow \infty$  at fixed  $(\alpha, \gamma)$ .

Readout distribution	Bayes-optimal error $\varepsilon^{\text{BO}}$	Effective width $k_c$
Dense	$\Theta(1)$	$\Theta(d)$
Power-law, $\beta < 1/2$	$\Theta(1)$	$\Theta(d)$
Power-law, $\beta = 1/2$	$\Theta(\frac{\ln \ln d}{\ln d})$	$\Theta(\frac{d}{\ln d})$
Power-law, $\beta > 1/2$	$\Theta(d^{\frac{1}{2\beta}-1})$	$\Theta(d^{\frac{1}{2\beta}})$
Exponentially decaying	$\Theta(\frac{\ln d}{d})$	$\Theta(\ln d)$
Ultra sparse	$\Theta(\frac{1}{d})$	$\Theta(1)$

Sparsity has a clear impact on the scaling of the error and effective width: delocalized readouts ( $\beta \leq 1/2$  or dense) saturate at  $\varepsilon^{\text{BO}} = \Theta(1)$  with  $k_c = \Theta(d)$  learnable features, while sparser readouts allow decay down to  $\Theta(1/d)$  due to a finite effective width for ultra-sparse ones. For dense readouts we independently recover the result of [6] in Appendix J; for power-law readouts we also characterize the limiting overlap profile.

## 4 Derivation of the main results

Our main results rely on a crucial statistical equivalence between the learning problem in the neural network model from the perspective of a single feature and a simpler “high-sample rate generalized linear model”; it is derived in Appendix B.

**Result 3.** *Let  $\sigma$  be a non-constant, non-even, differentiable function such that  $\sigma, \sigma'$  are square-integrable w.r.t. the standard Gaussian measure on  $\mathbb{R}$  (we do not need here to restrict to the case  $\mu_2 = 0$ ). Let  $n, d, \Delta$  be in the regime  $n \gg d \gg 1$ , and define  $\lambda := \frac{n}{d\Delta}$ . Consider the problem of inferring the signal  $\mathbf{w}^0 \sim \mathcal{U}(\mathbb{S}^{d-1})$  from the observations  $\mathbf{Y} = (y_\mu)_{\mu=1}^n$  given by:*

$$y_\mu = \sigma(\mathbf{w}^0 \cdot \mathbf{x}_\mu) + \sqrt{\Delta} z_\mu, \quad \mu \in [n], \quad (11)$$

with inputs  $\mathbf{x}_\mu \sim \mathcal{N}(0, \mathbf{I}_d)$  and i.i.d. noise variables  $z_\mu \sim \mathcal{N}(0, 1)$ . Let  $\mathbf{w}^1$  be a sample from the posterior  $P(\mathbf{w} \mid \mathbf{Y})$ . Then, recalling definitions (4), we have

$$\mathbb{E} \langle (\mathbf{w}^0 \cdot \mathbf{w}^1 - m_\sigma(\lambda))^2 \rangle = o_d(1). \quad (12)$$

In particular, when the information exponent of  $\sigma$  is at least 3 (Appendix A), the model exhibits a sharp phase transition at  $\lambda_\sigma$ :  $m_\sigma(\lambda) = 0$  if  $\lambda < \lambda_\sigma$ , whereas  $m_\sigma(\lambda) > 0$  if  $\lambda > \lambda_\sigma$  (Appendix D).

We now provide the main steps of our heuristic derivation of Result 1 based on the leave-one-out argument and Gaussian assumptions.

**Feature overlaps and Bayes-optimal error.** Recall that  $\langle \cdot \rangle$  denotes the posterior mean w.r.t.  $P(\mathbf{W} \mid \mathcal{D})$ , and  $\mathbf{W}^1$  is a posterior sample. Fix  $i \in [k]$ . The leave-one-out approach relies on isolating the contribution of feature  $\mathbf{w}_i^0$  in the model (1):

$$y_\mu^{\text{out}} = v_i \sigma(\mathbf{w}_i^0 \cdot \mathbf{x}_\mu) + R_{\mu i} + \sqrt{\Delta} z_\mu, \quad R_{\mu i} := \sum_{j \neq i} v_j \sigma(\mathbf{w}_j^0 \cdot \mathbf{x}_\mu). \quad (13)$$

Decompose  $R_{\mu i}$  into its posterior mean and a posterior fluctuation that acts as an effective noise:  $R_{\mu i} = \langle R_{\mu i} \rangle + (R_{\mu i} - \langle R_{\mu i} \rangle)$ . The posterior mean  $\langle R_{\mu i} \rangle$  is a deterministic function of the dataset  $\mathcal{D}$  that can be absorbed into the observation  $y_\mu^{\text{out}} \rightarrow y_\mu^{\text{out}} - \langle R_{\mu i} \rangle$  without changing the posterior. We thus focus on the effective noise, whose variance is  $\langle (R_{\mu i} - \langle R_{\mu i} \rangle)^2 \rangle \sim \sum_{j \neq i} v_j^2 (g_\sigma(1) - g_\sigma(q_j)) := \varepsilon_{-i}$ . This together with the relation below,

$$\varepsilon^{\text{BO}} \sim \sum_{i=1}^k v_i^2 (g_\sigma(1) - g_\sigma(q_i)) := \varepsilon. \quad (14)$$

are derived for a special case – and assumed to hold in general – in Appendix F. *We make the additional assumption that, with fixed  $i$  while  $\mu$  varies, the effective noises behave like independent Gaussian variables* – this central limit theorem heuristic, standard in the cavity method [37], was tested numerically and verified a-posteriori via the excellent match between our theory and experiments, as well as via the analytical match with the equations of [6] in the dense readout case. Combining the effective noise with the original label noise yields a single effective Gaussian noise of variance  $\Delta + \varepsilon_{-i}$ , so that (13) (after subtracting the deterministic  $\langle R_{\mu i} \rangle$ ) takes the form

$$\text{observation}_\mu = v_i \sigma (\mathbf{w}_i^0 \cdot \mathbf{x}_\mu) + \sqrt{\Delta + \varepsilon_{-i}} \text{noise}_\mu. \quad (15)$$

By Result 3,

$$\mathbf{w}_i^0 \cdot \mathbf{w}_i^1 \simeq m_\sigma \left( \frac{nv_i^2/d}{\Delta + \varepsilon_{-i}} \right) \simeq m_\sigma \left( \frac{nv_i^2/d}{\Delta + \varepsilon} \right) \quad (16)$$

where in the last step we used  $\Delta + \varepsilon_{-i} = \Delta + \varepsilon + O(1/k)$ . Together with the equation for  $\varepsilon$ , this closes the system of fixed-point equations (6).

**Asymptotic Bayes-optimal error.** From (14), and using  $q_i = 0$  for  $i > k_c$ , we have

$$\varepsilon^{\text{BO}} \sim \sum_{i \leq k_c} v_i^2 (g_\sigma(1) - g_\sigma(q_i)) + \sum_{k_c < i \leq k} v_i^2 g_\sigma(1).$$

The second sum, which is the error due to non-learnable features, is  $\Theta(\sum_{k_c < i \leq k} v_i^2)$ . On the other hand, from the fixed point equations (6), we have  $q_i = m_\sigma(\text{snr}_i)$ , where recall that  $\text{snr}_i = (n/d)v_i^2/(\Delta + \varepsilon)$ . For any  $i \leq k_c$ , feature  $i$  is learnable, so  $\text{snr}_i > \lambda_\sigma$ . The first sum becomes

$$(\Delta + \varepsilon) \frac{d}{n} \sum_{i \leq k_c} \text{snr}_i (g_\sigma(1) - g_\sigma \circ m_\sigma(\text{snr}_i)),$$

which is  $\Theta(k_c d/n)$ , since  $\Delta + \varepsilon = \Theta(1)$  and there exist absolute constants  $c_1, c_2 > 0$  such that  $x(g_\sigma(1) - g_\sigma \circ m_\sigma(x)) \in [c_1, c_2]$  for all  $x > \lambda_\sigma$  (Appendix D).

From the derivation, each learnable feature contributes  $\Theta(d/n)$  to the BO error, while each non-learnable feature  $i$  contributes  $\Theta(v_i^2)$ .

## 5 Conclusion and limitations

We studied the information-theoretic limits of learning a one-hidden-layer teacher network in the extensive-width regime  $k = \Theta(d)$ , a setting that captures large-but-finite-width networks and sits strictly between the multi-index and NTK/infinite-width extremes. We provided a heuristic leave-one-out argument yielding closed fixed-point equations for the individual feature overlaps ( $q_i$ ) and the Bayes-optimal error  $\varepsilon^{\text{BO}}$ . A single activation-dependent SNR threshold  $\lambda_\sigma$  governs feature learnability: as  $n$  grows, features cross it one by one, producing a staircase of sharp phase transitions in the learning curve. For a power-law hierarchy of features with exponent  $\beta > 1/2$ , the resulting effective width  $k_c \leq k$  unifies the two empirically observed scaling regimes via  $\varepsilon^{\text{BO}} = \Theta(k_c d/n)$ : a feature-learning regime in which  $k_c$  grows with  $n$ , and a refinement regime in which  $k_c = k$  is saturated and the parametric rate  $n^{-1}$  is recovered. An ADAM-trained student near  $k_c$  tracks these Bayes-optimal exponents up to a small residual gap on the weakest features, consistent with an algorithmic threshold  $\lambda_\sigma^{\text{algo}} > \lambda_\sigma$ .

The main limitations of our work are that derivations rest on unproved cavity assumptions – Gaussian cavity fields and overlap concentration – and the restriction  $\mu_2 = 0$ . Tackling general activations in the extensive-width regime  $k = \Theta(d)$  is a technical challenge that has been considered only recently [6]. Closing the  $\mu_2$  gap [20, 33], proving the leave-one-out reduction, extending to multi-layer architectures [6], and characterizing compute-optimal scaling [28] are natural next steps.

## Acknowledgments

J.B. and M.-T.N. were funded by the European Union (ERC, CHORAL, project number 101039794). Views and opinions expressed are however those of the authors only and do not necessarily reflect those of the European Union or the European Research Council. Neither the European Union nor the granting authority can be held responsible for them.

## References

- [1] Emmanuel Abbe, Enric Boix Adsera, and Theodor Misiakiewicz. Sgd learning on neural networks: leap complexity and saddle-to-saddle dynamics. In *The Thirty Sixth Annual Conference on Learning Theory*, pages 2552–2623. PMLR, 2023.
- [2] Gérard Ben Arous, Murat A Erdogdu, N Mert Vural, and Denny Wu. Learning quadratic neural networks in high dimensions: Sgd dynamics and scaling laws. *arXiv preprint arXiv:2508.03688*, 2025.
- [3] Gerard Ben Arous, Reza Gheissari, and Aukosh Jagannath. Online stochastic gradient descent on non-convex losses from high-dimensional inference. *Journal of Machine Learning Research*, 22(106):1–51, 2021.
- [4] Benjamin Aubin, Antoine Maillard, Florent Krzakala, Nicolas Macris, Lenka Zdeborová, et al. The committee machine: Computational to statistical gaps in learning a two-layers neural network. *Advances in Neural Information Processing Systems*, 31, 2018.
- [5] Yasaman Bahri, Ethan Dyer, Jared Kaplan, Jaehoon Lee, and Utkarsh Sharma. Explaining neural scaling laws. *Proceedings of the National Academy of Sciences*, 121(27):e2311878121, 2024.
- [6] Jean Barbier, Francesco Camilli, Minh-Toan Nguyen, Mauro Pastore, and Rudy Skerk. Statistical physics of deep learning: Optimal learning of a multi-layer perceptron near interpolation. *Physical Review X*, Apr 2026.
- [7] Jean Barbier, Florent Krzakala, Nicolas Macris, Léo Miolane, and Lenka Zdeborová. Optimal errors and phase transitions in high-dimensional generalized linear models. *Proceedings of the National Academy of Sciences*, 116(12):5451–5460, 2019.
- [8] Jean Barbier and Dmitry Panchenko. Strong replica symmetry in high-dimensional optimal bayesian inference. *Communications in mathematical physics*, 393(3):1199–1239, 2022.
- [9] Mohsen Bayati and Andrea Montanari. The dynamics of message passing on dense graphs, with applications to compressed sensing. *IEEE Transactions on Information Theory*, 57(2):764–785, 2011.
- [10] Blake Bordelon, Alexander Atanasov, and Cengiz Pehlevan. A dynamical model of neural scaling laws. In *International Conference on Machine Learning*, pages 4345–4382. PMLR, 2024.
- [11] Cristian Buciluă, Rich Caruana, and Alexandru Niculescu-Mizil. Model compression. In *Proceedings of the 12th ACM SIGKDD international conference on Knowledge discovery and data mining*, pages 535–541, 2006.
- [12] Francesco Cagnetta, Hyunmo Kang, and Matthieu Wyart. Learning curves theory for hierarchically compositional data with power-law distributed features. *arXiv preprint arXiv:2505.07067*, 2025.
- [13] Francesco Camilli, Daria Tieplova, Eleonora Bergamin, and Jean Barbier. Information-theoretic reduction of deep neural networks to linear models in the overparametrized proportional regime. In *The Thirty Eighth Annual Conference on Learning Theory*, pages 757–798. PMLR, 2025.
- [14] Lenaïc Chizat, Edouard Oyallon, and Francis Bach. On lazy training in differentiable programming. *Advances in neural information processing systems*, 32, 2019.

- [15] Hugo Cui, Bruno Loureiro, Florent Krzakala, and Lenka Zdeborová. Generalization error rates in kernel regression: The crossover from the noiseless to noisy regime. *Advances in Neural Information Processing Systems*, 34:10131–10143, 2021.
- [16] Alex Damian, Eshaan Nichani, Rong Ge, and Jason D Lee. Smoothing the landscape boosts the signal for sgd: Optimal sample complexity for learning single index models. *Advances in Neural Information Processing Systems*, 36:752–784, 2023.
- [17] Alex Damian, Loucas Pillaud-Vivien, Jason Lee, and Joan Bruna. Computational-statistical gaps in gaussian single-index models. In *The Thirty Seventh Annual Conference on Learning Theory*, pages 1262–1262. PMLR, 2024.
- [18] Alexandru Damian, Jason Lee, and Mahdi Soltanolkotabi. Neural networks can learn representations with gradient descent. In *Conference on Learning Theory*, pages 5413–5452. PMLR, 2022.
- [19] Leonardo Defilippis, Florent Krzakala, Bruno Loureiro, and Antoine Maillard. A noise sensitivity exponent controls large statistical-to-computational gaps in single-and multi-index models. *arXiv preprint arXiv:2603.17896*, 2026.
- [20] Leonardo Defilippis, Florent Krzakala, Bruno Loureiro, and Antoine Maillard. Optimal scaling laws in learning hierarchical multi-index models. *arXiv preprint arXiv:2602.05846*, 2026.
- [21] Leonardo Defilippis, Bruno Loureiro, and Theodor Misiakiewicz. Dimension-free deterministic equivalents and scaling laws for random feature regression. *Advances in Neural Information Processing Systems*, 37:104630–104693, 2024.
- [22] Leonardo Defilippis, Yizhou Xu, Julius Girardin, Emanuele Troiani, Vittorio Erba, Lenka Zdeborová, Bruno Loureiro, and Florent Krzakala. Scaling laws and spectra of shallow neural networks in the feature learning regime. *arXiv preprint arXiv:2509.24882*, 2025.
- [23] Nayara Fonseca, Seok Hyeong Lee, Chris Mingard, Ard Louis, et al. An exactly solvable model for emergence and scaling laws in the multitask sparse parity problem. *Advances in Neural Information Processing Systems*, 37:39632–39693, 2024.
- [24] Behrooz Ghorbani, Song Mei, Theodor Misiakiewicz, and Andrea Montanari. Linearized two-layers neural networks in high dimension. *The Annals of Statistics*, 49(2):1029–1054, 2021.
- [25] Jianping Gou, Baosheng Yu, Stephen J Maybank, and Dacheng Tao. Knowledge distillation: A survey. *International journal of computer vision*, 129(6):1789–1819, 2021.
- [26] Joel Hestness, Sharan Narang, Newsha Ardalani, Gregory Diamos, Heewoo Jun, Hassan Kianinejad, Md Mostofa Ali Patwary, Yang Yang, and Yanqi Zhou. Deep learning scaling is predictable, empirically. *arXiv preprint arXiv:1712.00409*, 2017.
- [27] Geoffrey Hinton, Oriol Vinyals, and Jeff Dean. Distilling the knowledge in a neural network. *arXiv preprint arXiv:1503.02531*, 2015.
- [28] Jordan Hoffmann, Sebastian Borgeaud, Arthur Mensch, Elena Buchatskaya, Trevor Cai, Eliza Rutherford, DDL Casas, Lisa Anne Hendricks, Johannes Welbl, Aidan Clark, et al. Training compute-optimal large language models. *arXiv preprint arXiv:2203.15556*, 10, 2022.
- [29] Marcus Hutter. Learning curve theory. *arXiv preprint arXiv:2102.04074*, 2021.
- [30] Arthur Jacot, Franck Gabriel, and Clément Hongler. Neural tangent kernel: Convergence and generalization in neural networks. *Advances in neural information processing systems*, 31, 2018.
- [31] Jared Kaplan, Sam McCandlish, Tom Henighan, Tom B Brown, Benjamin Chess, Rewon Child, Scott Gray, Alec Radford, Jeffrey Wu, and Dario Amodei. Scaling laws for neural language models. *arXiv preprint arXiv:2001.08361*, 2020.

- [32] Licong Lin, Jingfeng Wu, Sham M Kakade, Peter L Bartlett, and Jason D Lee. Scaling laws in linear regression: Compute, parameters, and data. *Advances in Neural Information Processing Systems*, 37:60556–60606, 2024.
- [33] Antoine Maillard, Emanuele Troiani, Simon Martin, Lenka Zdeborová, and Florent Krzakala. Bayes-optimal learning of an extensive-width neural network from quadratically many samples. *Advances in Neural Information Processing Systems*, 37:82085–82132, 2024.
- [34] Eric Michaud, Ziming Liu, Uzay Girit, and Max Tegmark. The quantization model of neural scaling. *Advances in Neural Information Processing Systems*, 36:28699–28722, 2023.
- [35] Elliot Paquette, Courtney Paquette, Lechao Xiao, and Jeffrey Pennington. 4+ 3 phases of compute-optimal neural scaling laws. *Advances in Neural Information Processing Systems*, 37:16459–16537, 2024.
- [36] Yunwei Ren, Eshaan Nichani, Denny Wu, and Jason D Lee. Emergence and scaling laws in SGD learning of shallow neural networks. *arXiv preprint arXiv:2504.19983*, 2025.
- [37] Michel Talagrand. *Mean field models for spin glasses: Volume I: Basic examples*, volume 54. Springer Science & Business Media, 2010.
- [38] Emanuele Troiani, Yatin Dandi, Leonardo DeFilippis, Lenka Zdeborova, Bruno Loureiro, and Florent Krzakala. Fundamental computational limits of weak learnability in high-dimensional multi-index models. In *International Conference on Artificial Intelligence and Statistics*, pages 2467–2475. PMLR, 2025.
- [39] Ge Yang, Edward Hu, Igor Babuschkin, Szymon Sidor, Xiaodong Liu, David Farhi, Nick Ryder, Jakub Pachocki, Weizhu Chen, and Jianfeng Gao. Tuning large neural networks via zero-shot hyperparameter transfer. *Advances in Neural Information Processing Systems*, 34:17084–17097, 2021.

## A Hermite expansion and information exponent

The  $\ell$ -th Hermite polynomial is defined as

$$\text{He}_\ell(x) := (-1)^\ell e^{x^2/2} \frac{d^\ell}{dx^\ell} e^{-x^2/2}, \quad \ell \geq 0. \quad (17)$$

$\text{He}_\ell$  is a polynomial of degree  $\ell$  with leading coefficient 1. A first few examples are  $\text{He}_0(x) = 1$ ,  $\text{He}_1(x) = x$ ,  $\text{He}_2(x) = x^2 - 1$ ,  $\text{He}_3(x) = x^3 - 3x$ . Any  $\sigma \in L^2(\mu)$  ( $\mu$  is the standard Gaussian measure) admits the *Hermite expansion*

$$\sigma(z) = \sum_{\ell=0}^{\infty} \frac{\mu_\ell}{\ell!} \text{He}_\ell(z), \quad (18)$$

in which the  $\ell$ -th *Hermite coefficient* of  $\sigma$  is given by  $\mu_\ell = \mathbb{E}_{z \sim \mathcal{N}(0,1)} \sigma(z) \text{He}_\ell(z)$ .

An important quantity is the *information exponent* of  $\sigma$  [3], defined as

$$k_\star(\sigma) := \min\{\ell \geq 1 : \mu_\ell \neq 0\}. \quad (19)$$

## B Heuristic derivation of Result 3

We provide here a heuristic derivation of Result 3. We start by deriving the fixed point equation for  $m_\sigma(\lambda)$ . Assuming  $\mathbf{w}^0 \cdot \mathbf{w}^1 \simeq q$  where  $\mathbf{w} = \mathbf{w}^1$  is a posterior sample, we will show that  $q/(1-q) = \lambda g'_\sigma(q)$ . Fix  $i \in [d]$  and focus on the estimation of  $w_i^0$

$$\bar{y}_\mu = \sigma(w_i^0 x_{\mu i} + A_{\mu i}) + \sqrt{\Delta} z_\mu, \quad \mu \in [n],$$

where  $A_{\mu i} = \sum_{j \neq i} w_j^0 x_{\mu j}$ . Since  $w_i^0 x_{\mu i}$  is small compared to  $A_{\mu i}$ , we can expand the model around  $A_{\mu i}$  and obtain

$$y_\mu \simeq \sigma(A_{\mu i}) + \sigma'(A_{\mu i}) w_i^0 x_{\mu i} + \sqrt{\Delta} z_\mu, \quad \mu \in [n].$$

We claim that  $\sigma(A_{\mu i})$  and  $\sigma'(A_{\mu i})$  can be replaced by their posterior averages  $\langle \sigma(A_{\mu i}) \rangle$  and  $\langle \sigma'(A_{\mu i}) \rangle$ : the fluctuations around the average contribute additional noise, negligible against the channel noise with variance  $\Delta$ . This is because, if  $\Delta = \Theta(1)$ , then since  $n \gg d$ , the overlap for  $\mathbf{w}^0$  is almost 1, making the fluctuations of  $\sigma(A_{\mu i})$  and  $\sigma'(A_{\mu i})$  of order  $o(1)$ , and thus negligible compared to  $\Delta$ . On the other hand, if  $\Delta \gg 1$ , since the fluctuations of  $\sigma(A_{\mu i})$  and  $\sigma'(A_{\mu i})$  are bounded, they remain negligible compared to  $\Delta$ .

Subtracting  $\langle \sigma(A_{\mu i}) \rangle$  yields the effective scalar model

$$\tilde{y}_\mu = \langle \sigma'(A_{\mu i}) \rangle w_i^0 x_{\mu i} + \sqrt{\Delta} \tilde{z}_\mu, \quad \mu \in [n],$$

which is equivalent to a single Gaussian channel for  $w_i^0$  with effective signal-to-noise ratio

$$r_i := \frac{1}{\Delta} \sum_{\mu=1}^n \langle \sigma'(A_{\mu i}) \rangle^2 x_{\mu i}^2.$$

Suppose that  $r_i$  concentrates around its mean. Using  $\mathbb{E}[x_{\mu i}^2] = 1$  together with the approximate independence between  $x_{\mu i}^2$  and  $\langle \sigma'(A_{\mu i}) \rangle$ , then replacing  $A_{\mu i}$  by  $\mathbf{w} \cdot \mathbf{x}_\mu$  inside the bracket (an  $O(d^{-1/2})$  correction), we obtain

$$\mathbb{E}[r_i] \sim \frac{n}{\Delta} \mathbb{E}[\langle \sigma'(\mathbf{w} \cdot \mathbf{x}_\mu) \rangle^2] = \lambda d \mathbb{E}[\langle \sigma'(\mathbf{w} \cdot \mathbf{x}_\mu) \rangle^2].$$

*Computing*  $\mathbb{E}[\langle \sigma'(\mathbf{w} \cdot \mathbf{x}_\mu) \rangle^2]$ . By Lemma 4 below,

$$\mathbf{w} \cdot \mathbf{x}_\mu \stackrel{(d)}{\simeq} \langle \mathbf{w} \cdot \mathbf{x}_\mu \rangle + \sqrt{1-q} \xi, \quad \xi \stackrel{\text{i.i.d.}}{\sim} \mathcal{N}(0, 1).$$

Since  $\mathbf{x}_\mu \sim \mathcal{N}(0, \mathbf{I}_d)$ , the average term is Gaussian with variance  $\|\langle \mathbf{w} \rangle\|^2 \simeq q$ . We obtain

$$\mathbf{w} \cdot \mathbf{x}_\mu \stackrel{(d)}{\simeq} \sqrt{q} \xi_0 + \sqrt{1-q} \xi_1, \quad \xi_0, \xi_1 \stackrel{\text{i.i.d.}}{\sim} \mathcal{N}(0, 1),$$

where  $\xi_0$  is measurable with respect to the data and  $\xi_1$  captures the posterior uncertainty. We obtain

$$\mathbb{E}[\langle \sigma'(\mathbf{w} \cdot \mathbf{x}_\mu) \rangle^2] \simeq \mathbb{E}_{\xi_0}(\mathbb{E}_{\xi_1} \sigma'(\sqrt{q}\xi_0 + \sqrt{1-q}\xi_1))^2 = g_{\sigma'}(q) = g'_\sigma(q)$$

where the second equality follows from Proposition 5.

Summarizing the previous arguments, for each  $i$ , the posterior of  $w_i$  is asymptotically that of a Gaussian channel with signal  $w_i^0$  and SNR  $\lambda d g'_\sigma(q)$ . Assuming independence across individual channels, the posterior of  $\mathbf{w}$  is asymptotically that of a Gaussian channel with signal  $\mathbf{w}^0$  and the same SNR. This channel admits a simple SNR-overlap relation,  $\text{snr}/d = q/(1-q)$ , yielding the fixed point equation

$$q/(1-q) = \lambda g'_\sigma(q).$$

This equation may have multiple solutions and thus does not uniquely determine  $q$ . A unique characterization of the overlap is instead achieved by maximizing a large deviation rate function  $I(q)$ , defined informally via

$$\frac{1}{d} \ln \mathbb{P}(\mathbf{w}^0 \cdot \mathbf{w}^1 \simeq q) \simeq I(q).$$

The fixed point equation is then simply  $I'(q) = 0$ . Integrating both sides of  $q/(1-q) - \lambda g'_\sigma(q) = 0$  suggests that, up to an affine transform, the rate function is

$$\lambda g_\sigma(q) + q + \ln(1-q), \quad (20)$$

which yields the unique characterization of the overlap given by  $m_\sigma(\lambda)$  via its argmax. Importantly, this integration argument relies on the specific form of the fixed point equation: the left-hand side  $q/(1-q)$  has a clear interpretation as the SNR of a Gaussian channel expressed in terms of the overlap, and it is this structure that makes this work. Note that integrating arbitrary equivalent form of the fixed point equation, such as  $q = (1-q)\lambda g'_\sigma(q)$ , does not recover the correct rate function. The resulting function (20) is called a ‘‘replica symmetric potential’’ in physics parlance, and can also be guessed by taking the joint high-sample-rate, high-noise limit, i.e.  $\alpha = n/d \rightarrow \infty$  and  $\Delta \rightarrow \infty$  with  $\alpha/\Delta \rightarrow \lambda$  fixed, in the replica symmetric potential for the standard generalized linear model [7].

**Lemma 4.** (informal result by Talagrand [37], Chapter 1.5) Consider a probability measure  $\mu = \mu_d$  in  $\mathbb{R}^d$ . Denote  $\langle \cdot \rangle$  the average with respect to  $\mu$ . Suppose there exist  $q$  and  $\rho$  such that for large  $d$ :

$$\langle (\mathbf{w}^1 \cdot \mathbf{w}^2 - q)^2 \rangle = o_d(1) \quad (21)$$

$$\langle (\|\mathbf{w}\|^2 - \rho)^2 \rangle = o_d(1). \quad (22)$$

Let  $\mathbf{x} \sim \mathcal{N}(0, \mathbf{I}_d)$  independent of  $\mu$ . Then

$$\mathbf{w} \cdot \mathbf{x} \stackrel{(d)}{\simeq} \langle \mathbf{w} \cdot \mathbf{x} \rangle + \sqrt{1-q} \xi, \quad \xi \stackrel{\text{i.i.d.}}{\sim} \mathcal{N}(0, 1).$$

We applied this lemma when  $\mu$  is the posterior distribution in the current model. The conditions (21) and (22) are satisfied by high-dimensional posterior distributions in more general settings of optimal Bayesian inference, as shown in [8].

## C Estimating the linear part via linear regression

We provide here the justification that the activation  $\sigma(x)$  can be replaced by  $\sigma(x) - \mu_0 - \mu_1 x$  without changing the asymptotic behavior of the posterior.

Without loss of generality, we can assume that  $\mu_0 = 0$ , since this is a constant that can be subtracted from  $y_\mu^{\text{out}}$ . We will show that  $\mathbf{s}^0 = \mathbf{W}^{0\top} \mathbf{v}$  can be estimated with vanishing error with the following estimator

$$\hat{\mathbf{s}} = \frac{1}{n\mu_1} \mathbf{X} \mathbf{y}. \quad (23)$$

Writing  $\mathbf{y}$  as

$$\mathbf{y} = \mu_1 \mathbf{X}^\top \mathbf{s}^0 + \boldsymbol{\xi}, \quad \boldsymbol{\xi} = \mathbf{v}^\top \bar{\sigma}(\mathbf{W}^0 \mathbf{X}) + \sqrt{\Delta} \mathbf{z},$$

we have

$$\hat{\mathbf{s}} = \frac{1}{n} \mathbf{X} \mathbf{X}^\top \mathbf{s}^0 + \frac{1}{n \mu_1} \mathbf{X} \boldsymbol{\xi}.$$

Since  $n \gg d$ , we have  $\mathbf{X} \mathbf{X}^\top / n \simeq \mathbf{I}_d$  which is a basic property of Wishart matrices. Therefore

$$\frac{1}{n} \mathbf{X} \mathbf{X}^\top \mathbf{s}^0 \simeq \mathbf{s}^0. \quad (24)$$

On the other hand,

$$\begin{aligned} \frac{1}{n} \mathbf{X} \boldsymbol{\xi} &= \frac{1}{n} \sum_{\mu=1}^n \xi_\mu \mathbf{x}_\mu \\ &\simeq \mathbb{E}_{\mathbf{x}, z} [(\mathbf{v}^\top \tilde{\sigma}(\mathbf{W}^0 \mathbf{x}) + \sqrt{\Delta} z) \mathbf{x}], \quad \text{since } n \gg d \\ &= \mathbb{E}_{\mathbf{x}} [(\mathbf{v}^\top \tilde{\sigma}(\mathbf{W}^0 \mathbf{x})) \mathbf{x}], \quad \text{since } \mathbb{E}[\mathbf{x} z] = 0 \\ &= \sum_{i=1}^k v_i \mathbb{E}[\tilde{\sigma}(\mathbf{w}_i^0 \cdot \mathbf{x}) \mathbf{x}]. \end{aligned}$$

Recall the following basic property of Hermite polynomials, where

$$\mathbb{E}[\text{He}_\ell(z_1) \text{He}_{\ell'}(z_2)] = 0$$

for all  $\ell \neq \ell'$  and  $(z_1, z_2)$  jointly Gaussian, each with variance 1. This implies  $\mathbb{E}[\tilde{\sigma}(\mathbf{w}_i^0 \cdot \mathbf{x}) x_j] = 0$ , or  $\mathbb{E}[\tilde{\sigma}(\mathbf{w}_i^0 \cdot \mathbf{x}) \mathbf{x}] = 0$ . Therefore

$$\frac{1}{n} \mathbf{X} \boldsymbol{\xi} \simeq 0. \quad (25)$$

Combining (24) and (25),  $\hat{\mathbf{s}} \simeq \mathbf{s}^0$ , so the linear contribution can be perfectly estimated and removed; the residual posterior on  $\mathbf{W}_0$  then matches that of the model with  $\tilde{\sigma}$  in place of  $\sigma$ .

## D Properties of $g_\sigma$ and $m_\sigma$

**Proposition 5.** *Let be a non-constant, differentiable function and assume  $\sigma, \sigma' \in L^2(\mu)$ . Then the functions  $g_\sigma$  and  $m_\sigma$  defined in (3), (4) satisfy the following properties:*

1.  $g_\sigma$  has the expansion

$$g_\sigma(x) = \sum_{\ell=0}^{\infty} \frac{\mu_\ell^2}{\ell!} x^\ell \quad (26)$$

where  $\mu_\ell = \mathbb{E}_{z \sim \mathcal{N}(0,1)}[\sigma(z) \text{He}_\ell(z)]$  is the  $\ell$ -th Hermite coefficient of  $\sigma$ . As a consequence,  $g_\sigma$  is strictly increasing in  $[0, 1]$ .

2.  $m_\sigma$  is non-decreasing,  $1 - m_\sigma(x) \sim c/x$  as  $x \rightarrow \infty$  for some constant  $c > 0$ . Consequently, there exists  $c_1, c_2 > 0$  such that  $x(g_\sigma(1) - g_\sigma \circ m_\sigma(x)) \in [c_1, c_2]$  for all  $x > \lambda_\sigma$

3. If  $k_\star(\sigma) \geq 3$ , there exists  $\lambda_\sigma > 0$ ,  $q_\sigma > 0$  such that  $m_\sigma(\lambda) = 0$  if  $\lambda < \lambda_\sigma$  and  $\lim_{\lambda \rightarrow \lambda_\sigma^+} m_\sigma(\lambda) = q_\sigma$ .

4.  $g'_\sigma = g_{\sigma'}$ .

*Proof.* 1. Recall Mehler's formula: for  $(z_1, z_2)$  a centered Gaussian vector with unit variances and correlation  $x \in [-1, 1]$ ,

$$\mathbb{E}[\text{He}_\ell(z_1) \text{He}_m(z_2)] = \delta_{\ell m} \ell! x^\ell, \quad \ell, m \geq 0. \quad (27)$$

Writing  $\sigma = \sum_{\ell \geq 0} \frac{\mu_\ell}{\ell!} \text{He}_\ell$  in  $L^2(\mu)$  and using the orthogonality (27), we obtain, for every  $x \in [-1, 1]$ ,

$$g_\sigma(x) = \mathbb{E}[\sigma(z_1) \sigma(z_2)] = \sum_{\ell, m \geq 0} \frac{\mu_\ell \mu_m}{\ell! m!} \mathbb{E}[\text{He}_\ell(z_1) \text{He}_m(z_2)] = \sum_{\ell \geq 0} \frac{\mu_\ell^2}{\ell!} x^\ell.$$

Justification of the interchange: we have

$$\sum_{\ell, m} \frac{|\mu_\ell \mu_m|}{\ell! m!} |\mathbb{E}[\text{He}_\ell(z_1) \text{He}_m(z_2)]| = \sum_{\ell} \frac{\mu_\ell^2}{\ell!} |x|^\ell \leq \sum_{\ell} \frac{\mu_\ell^2}{\ell!} = \|\sigma\|_{L^2(\mu)}^2 < \infty$$

for  $|x| \leq 1$ , so Fubini applies. The series (26) therefore converges absolutely on  $[-1, 1]$ , and in particular at  $x = 1$ .

2. Recall that

$$m_\sigma(\lambda) = \arg \max_{q \in (0,1)} F(\lambda, q), \quad F(\lambda, q) = \lambda g_\sigma(q) + q + \ln(1 - q).$$

*Monotonicity.* Consider  $\lambda_1 > \lambda_2 \geq 0$ . Let  $q_1 = m_\sigma(\lambda_1)$ ,  $q_2 = m_\sigma(\lambda_2)$ . By optimality of  $q_1$  and  $q_2$ ,

$$\begin{aligned} F(\lambda_1, q_1) &\geq F(\lambda_1, q_2), \\ F(\lambda_2, q_2) &\geq F(\lambda_2, q_1). \end{aligned}$$

Adding the two inequalities and simplifying,

$$(\lambda_1 - \lambda_2)(g_\sigma(q_1) - g_\sigma(q_2)) \geq 0.$$

Since  $\lambda_1 > \lambda_2$ , this implies  $g_\sigma(q_1) \geq g_\sigma(q_2)$ . Since  $g_\sigma$  is strictly increasing (Part 1), we have  $q_1 \geq q_2$ . We conclude that  $m_\sigma$  is non-decreasing in  $[0, \infty)$ .

*Asymptotic behavior.* Let  $q = m_\sigma(\lambda)$ . Then  $q$  satisfies  $q/(1 - q) = \lambda g'_\sigma(q)$ . When  $\lambda \rightarrow \infty$ , we have  $q \rightarrow 1$ . From  $q = (1 - q)\lambda g'_\sigma(q)$ , as  $\lambda \rightarrow \infty$ , we have  $1 \sim (1 - q)\lambda g'_\sigma(1)$ , which gives  $m_\sigma(\lambda) = q \sim 1 - c/\lambda$ , where  $c = 1/g'_\sigma(1)$ .

*Boundedness of  $\kappa(x) := x(g_\sigma(1) - g_\sigma \circ m_\sigma(x))$  on  $(\lambda_\sigma, \infty)$ .* From the asymptotic of  $m_\sigma$ , we have  $\kappa(x) \rightarrow 1$  as  $x \rightarrow \infty$ . Fix a  $\epsilon > 0$ . There exists  $M > 0$  such that  $\kappa(x) \in [1 - \epsilon, 1 + \epsilon]$  for all  $x \geq M$ . For  $x \in (\lambda_\sigma, M]$ ,  $\kappa(x)$  is bounded above by  $M g_\sigma(1)$  and bounded below by  $\lambda_\sigma(g_\sigma(1) - g_\sigma \circ m_\sigma(M)) > 0$ .

3. We first observe that  $q = 0$  is always a local maximum of  $F(\lambda, q)$  for every  $\lambda \geq 0$ . Indeed, we have

$$\partial_q^2 F(\lambda, q) = \lambda g''_\sigma(q) - \frac{1}{(1 - q)^2},$$

which gives  $\partial_{q=0}^2 F(\lambda, q) = -1 < 0$ , since  $g''_\sigma(0) = 0$  as  $k_*(\sigma) \geq 3$ . Next,  $q = 0$  is the global maximum if and only if

$$\lambda g_\sigma(q) + q + \ln(1 - q) < 0, \quad \forall q \in (0, 1),$$

which is equivalent to

$$\lambda < \lambda_\sigma := \inf_{q \in (0,1)} h(q), \quad h(q) = \frac{-q - \ln(1 - q)}{g_\sigma(q)}. \quad (28)$$

Let  $q_\sigma = \arg \inf_{q \in (0,1)} h(q)$ . Since  $h(q) > 0$  for all  $q \in (0, 1)$ ,  $\lim_{q \rightarrow 0^+} h(q) = \lim_{q \rightarrow 1^-} h(q) = \infty$ , it follows that  $q_\sigma, \lambda_\sigma$  are well-defined and  $\lambda_\sigma \in (0, \infty)$ . It also follows from the definition of  $q_\sigma$  that  $\lim_{\lambda \rightarrow \lambda_\sigma^+} m_\sigma(\lambda) = q_\sigma$ .

4. Expand

$$\sigma(z) = \sum_{\ell \geq 0} a_\ell \text{He}_\ell(z), \quad a_\ell = \mu_\ell / \ell!.$$

Using  $\text{He}'_\ell(z) = \ell \text{He}_{\ell-1}(z)$  and the assumption  $\sigma' \in L^2(\mu)$  (so the term-by-term differentiation is justified in  $L^2$ ), we obtain

$$\sigma'(z) = \sum_{\ell \geq 1} a_\ell \ell \text{He}_{\ell-1}(z).$$

Mehler's formula gives

$$\mathbb{E}[\text{He}_\ell(z_1) \text{He}_m(z_2)] = \delta_{\ell m} \ell! x^\ell \quad \text{for} \quad (z_1, z_2) \sim \mathcal{N}\left(0, \begin{bmatrix} 1 & x \\ x & 1 \end{bmatrix}\right).$$

Therefore,

$$g_\sigma(x) = \mathbb{E}[\sigma(z_1)\sigma(z_2)] = \sum_{\ell \geq 0} a_\ell^2 \ell! x^\ell,$$

so

$$g'_\sigma(x) = \sum_{\ell \geq 1} a_\ell^2 \ell! \ell x^{\ell-1}.$$

On the other hand,

$$g_{\sigma'}(x) = \mathbb{E}[\sigma'(z_1)\sigma'(z_2)] = \sum_{\ell \geq 1} a_\ell^2 \ell^2 (\ell-1)! x^{\ell-1} = \sum_{\ell \geq 1} a_\ell^2 \ell! \ell x^{\ell-1}.$$

Hence  $g'_\sigma(x) = g_{\sigma'}(x)$  for  $x \in [0, 1]$ .  $\square$

## E Proof of features decoupling in the dense readouts case

Let us prove the neuron decoupling – first identity in (5) – for the special case  $\sqrt{k}\mathbf{v} = \mathbf{1}$ ; we conjecture that this strategy with additional care extends to more general readout distributions. We have

$$\begin{aligned} \sum_{i,j=1}^k \mathbb{E}\langle (\mathbf{w}_i^0 \cdot \mathbf{w}_j^1)^2 \rangle &= \mathbb{E}\left\langle \sum_{i,j=1}^k \sum_{l,m=1}^d w_{il}^0 w_{jl}^1 w_{im}^0 w_{jm}^1 \right\rangle \\ &= \mathbb{E}\left\langle \sum_{l,m} [\mathbf{W}^{0\top} \mathbf{W}^0]_{lm} [\mathbf{W}^{1\top} \mathbf{W}^1]_{lm} \right\rangle \\ &= \mathbb{E}\langle \text{Tr}(\mathbf{W}^{0\top} \mathbf{W}^0 \mathbf{W}^{1\top} \mathbf{W}^1) \rangle \\ &\leq \sqrt{\mathbb{E}\langle \|\mathbf{W}^{0\top} \mathbf{W}^0\|_F^2 \rangle \mathbb{E}\langle \|\mathbf{W}^{1\top} \mathbf{W}^1\|_F^2 \rangle} \\ &= \mathbb{E}\|\mathbf{W}^{0\top} \mathbf{W}^0\|_F^2 = \mathbb{E}\|\mathbf{W}^0 \mathbf{W}^{0\top}\|_F^2 = k. \end{aligned}$$

This sum contains  $k$  equal terms of order  $O(1)$  and other  $k(k-1)$  “off-diagonal” terms that are equal by statistical exchangeability. This implies that the off-diagonal terms are of order  $O(k^{-1}) = O(d^{-1})$  as claimed.

## F More details on the derivation of the main result

We fill in some details of the derivation of the main result. First, we show that

$$\varepsilon^{\text{BO}} \sim \sum_{i=1}^k v_i^2 (g_\sigma(1) - g_\sigma(q_i)) \quad (29)$$

holds in the dense readout, interpolation regime, while leaving a complete proof for future work.

Since the BO error is half of Gibbs error, we have

$$\varepsilon^{\text{BO}} = \frac{1}{2} \mathbb{E}_{\mathcal{D}, \mathbf{W}, \mathbf{W}^1} \mathbb{E}_{\mathbf{x} \sim \mathcal{N}(0, \mathbf{I}_d)} [(y_1 - y_0)^2]$$

where

$$y_0 = \mathbf{v}^\top \sigma(\mathbf{W}^0 \mathbf{x}), \quad y_1 = \mathbf{v}^\top \sigma(\mathbf{W}^1 \mathbf{x})$$

and  $\mathbf{W}^1$  is drawn from the posterior  $P(\mathbf{W} | \mathcal{D})$ . We have

$$\begin{aligned} \mathbb{E}_{\mathbf{x}}[(y_1 - y_0)^2] &= \mathbb{E}_{\mathbf{x}}[y_0^2] + \mathbb{E}_{\mathbf{x}}[y_1^2] - 2\mathbb{E}[y_0 y_1] \\ \mathbb{E}_{\mathbf{x}}[y_1^2] = \mathbb{E}_{\mathbf{x}}[y_0^2] &= \sum_{i,j=1}^k v_i v_j \mathbb{E}_{\mathbf{x}}[\sigma(\mathbf{w}_i^0 \cdot \mathbf{x}) \sigma(\mathbf{w}_j^0 \cdot \mathbf{x})] = \sum_{i,j=1}^k v_i v_j g_\sigma(\mathbf{w}_i^0 \cdot \mathbf{w}_j^0) = g_\sigma(1) \\ \mathbb{E}_{\mathbf{x}}[y_0 y_1] &= \sum_{i,j=1}^k v_i v_j \mathbb{E}_{\mathbf{x}}[\sigma(\mathbf{w}_i^0 \cdot \mathbf{x}) \sigma(\mathbf{w}_j^1 \cdot \mathbf{x})] = \sum_{i,j=1}^k v_i v_j g_\sigma(\mathbf{w}_i^0 \cdot \mathbf{w}_j^1). \end{aligned}$$

Sue to the concentration of  $\mathbb{E}_{\mathbf{x}}[(y_0 - y_1)^2]$  with respect to  $(\mathcal{D}, \mathbf{W}^0, \mathbf{W}^1)$ , and since  $B$  is negligible compared to  $A$ , we have

$$\varepsilon^{\text{BO}} \sim \frac{1}{2} \mathbb{E}_{\mathbf{x}}[(y_0 - y_1)^2] = \underbrace{\sum_{i=1}^k v_i^2 (g_\sigma(1) - g_\sigma(\mathbf{w}_i^0 \cdot \mathbf{w}_i^1))}_A - \underbrace{\sum_{i \neq j} v_i v_j g_\sigma(\mathbf{w}_i^0 \cdot \mathbf{w}_j^1)}_B$$

It suffices to show that  $B$  is negligible compared to  $\varepsilon^{\text{BO}}$ , since this implies

$$\varepsilon^{\text{BO}} \sim A \sim \sum_{i=1}^k v_i^2 (g_\sigma(1) - g_\sigma(q_i))$$

Since  $g_\sigma(x) = O(x^3)$  when  $k_*(\sigma) \geq 3$ , each  $g_\sigma(\mathbf{w}_i^0 \cdot \mathbf{w}_j^1)$ , with  $i \neq j$ , is of order  $d^{-3/2}$ . Moreover, when  $\mathbf{v}$  is dense, the entries  $v_i$  are of order  $k^{-1/2}$ , it follows that  $B = O(kd^{-3/2}) = O(d^{-1/2})$ . In the dense readout, interpolation regime,  $\varepsilon^{\text{BO}} = \Theta(1)$ . We conclude  $B \ll \varepsilon^{\text{BO}}$ .

The derivation for the variance of  $R_{\mu i}$  follows verbatim, since  $R_{\mu i}$  only differs from  $\mathbf{v}^\top \sigma(\mathbf{W} \mathbf{x}_\mu)$  by a single term  $v_i \sigma(\mathbf{w}_i^0 \cdot \mathbf{x}_\mu)$ .

For general case, we give here some insights that may help to prove (29). Let us denote  $Q_{ij} := \mathbf{w}_i^0 \cdot \mathbf{w}_j^1$ .

1.  $\sum_i Q_{ij}^2 = \sum_j Q_{ij}^2 = 1$ . This identity is useful for bounding  $B$  when  $n$  is very large, as in this regime the overlaps  $Q_{ii} \simeq q_i$  are close to 1, which suppresses the off-diagonal terms.
2. Experimentally, we observe that  $Q_{ij}$  for  $i \neq j$  are *asymptotically uncorrelated*, i.e.

$$\text{Var}(B) \lesssim \sum_{i \neq j} v_i^2 v_j^2 \text{Var}(Q_{ij}^3),$$

This improves upon the pessimistic upper bound we used in the dense readout, interpolation regime.

## G Optimal scaling laws for $\beta > 1/2$

Recall that the effective SNR for feature  $i$  is

$$\text{snr}_i = \frac{(n/d)v_i^2}{\Delta + \varepsilon^{\text{BO}}}.$$

Consequently, the weakest feature (indexed by  $k$ ) is learnable whenever  $\text{snr}_k > \lambda_\sigma$ , which in turn requires  $n \gtrsim k^{2\beta} d$ . Using  $k^{2\beta} d$  as the threshold, we distinguish two regimes for  $n$ , in addition to the standing assumption that  $n \gg d$ :

- When  $n \ll k^{2\beta} d$ , the weakest feature is not learnable, so  $k_c < k$ . From

$$\text{snr}_{k_c} > \lambda_\sigma > \text{snr}_{k_c+1} \quad \text{i.e.} \quad \frac{(n/d)v_{k_c}^2}{\Delta + \varepsilon^{\text{BO}}} > \lambda_\sigma > \frac{(n/d)v_{k_c+1}^2}{\Delta + \varepsilon^{\text{BO}}},$$

we obtain  $k_c = \Theta((n/d)^{1/(2\beta)})$ , which implies  $1 \ll k_c \ll k$ . Recall from Result 1,

$$\varepsilon^{\text{BO}} = \Theta\left(\frac{k_c d}{n}\right) + \Theta\left(\sum_{i > k_c} v_i^2\right).$$

From the asymptotics of  $k_c$ , the first term in this decomposition is  $\Theta((n/d)^{1/(2\beta)-1})$ . On the other hand,

$$\begin{aligned} \sum_{i > k_c} v_i^2 &= \Theta\left(\sum_{i > k_c} i^{-2\beta}\right) = \Theta\left(\int_{k_c}^k x^{-2\beta} dx\right) \\ &= \Theta\left(k_c^{1-2\beta} - k^{1-2\beta}\right) = \Theta\left(k_c^{1-2\beta}\right) \\ &= \Theta((n/d)^{1/(2\beta)-1}). \end{aligned}$$

Thus, the second term in the decomposition is comparable to the first one. We conclude  $\varepsilon^{\text{BO}} = \Theta((n/d)^{1/(2\beta)-1})$ , which scales as  $n^{\frac{1}{2\beta}-1}$  when  $k, d$  are fixed.

- When  $n \gg k^{2\beta}d$ , all the features are learnable:  $k_c = k$ . The second term in the error decomposition vanishes, so  $\varepsilon^{\text{BO}} = \Theta(kd/n)$ , which scales as  $n^{-1}$  for fixed  $k, d$ .

It is worth noting from the preceding argument that when  $d \ll n \ll k^{2\beta}d$ , the first term in the error decomposition is comparable to the second. As  $n$  increases, additional features become learnable, causing the first term to grow while the second decreases. Consequently, as long as  $n \gg d$ , the second term is either comparable to or negligible relative to the first. Therefore, the asymptotics for Bayes-optimal error simplifies to  $\Theta(k_c d/n)$  for all  $n \gg d$ .

## H Extensive-width, near-interpolation regime

We derive here the results in the table of Section 3. Recall that in the interpolation regime, we have  $k \sim \gamma d$  and  $n \sim \alpha d^2$ , where  $\gamma, \alpha > 0$  are fixed parameters.

**Ultra-sparse readout.** In this case, the vector  $\mathbf{v}$  has only finitely many nonzero components. Assume  $v_1 \geq \dots \geq v_p > 0$  with  $p = \Theta(1)$ , while  $v_{p+1} = \dots = v_k = 0$ . For  $i \leq p$ , recall that the effective signal-to-noise ratio of  $\mathbf{w}_i$  is  $\text{snr}_i = (n/d)v_i^2/(\Delta + \varepsilon^{\text{BO}})$ . Since  $v_i = \Theta(1)$  and  $\Delta = \Theta(1)$ , it follows that  $\text{snr}_i \gg 1$ . Therefore, feature  $i$  is learnable for every  $i \leq p$ , implying  $k_c = p = \Theta(1)$ . Using (7), we obtain  $\varepsilon^{\text{BO}} = \Theta(k_c d/n) = \Theta(d/n) = \Theta(d^{-1})$ .

For the remaining readout cases (dense, power-law, and exponentially decayed), recall that when  $k_c < k$ ,

$$\frac{(n/d)v_{k_c}^2}{\Delta + \varepsilon^{\text{BO}}} > \lambda_\sigma > \frac{(n/d)v_{k_c+1}^2}{\Delta + \varepsilon^{\text{BO}}}$$

In each of these cases, consecutive readout coefficients satisfy  $v_i/v_{i+1} = \Theta(1)$ . Combined with  $\Delta = \Theta(1)$ , the above inequality yields

$$v_{k_c}^2 = \Theta\left(\frac{d}{n}\right) = \Theta\left(\frac{1}{d}\right) \quad (30)$$

Now let us deal with each case

**Power-law,  $\beta > 1/2$ .** In this case  $v_i^2 = \Theta(i^{-2\beta})$ . Combined with (30), this gives  $k_c = \Theta(d^{\frac{1}{2\beta}})$ . From Result 1,

$$\varepsilon^{\text{BO}} = \Theta\left(\frac{k_c d}{n}\right) + \Theta\left(\sum_{i>k_c} v_i^2\right). \quad (31)$$

By the asymptotics of  $k_c$ , both terms on the right-hand side are  $\Theta(d^{\frac{1}{2\beta}-1})$ , and we conclude that  $\varepsilon^{\text{BO}} = \Theta(d^{\frac{1}{2\beta}-1})$ .

**Power-law,  $\beta < 1/2$ .** We have  $v_i^2 = \Theta(i^{-2\beta}k^{2\beta-1})$ . Combined with (30), this gives  $k_c = \Theta(d)$ , so the first term in (31) is  $\Theta(1)$  and the second term is  $O(1)$ . We conclude  $\varepsilon^{\text{BO}} = \Theta(1)$ .

**Power-law,  $\beta = 1/2$ .** We have  $v_i^2 = \Theta(i^{-1}/\ln k)$ . Combined with (30), this gives  $k_c = \Theta(d/\ln d)$ , so the first term in (31) is  $\Theta(\frac{1}{\ln d})$  while the second term is  $\Theta(\frac{\ln \ln d}{\ln d})$ . We conclude  $\varepsilon^{\text{BO}} = \Theta(\frac{\ln \ln d}{\ln d})$ .

**Exponentially decaying.** We have  $v_i = \Theta(e^{-ci})$  for some constant  $c > 0$ . Combined with (30), this gives  $k_c = \Theta(\ln d)$ . The first term in (31) dominates, and we conclude  $\varepsilon^{\text{BO}} = \Theta(\frac{\ln d}{d})$ .

## I Additional simulations

The plots of  $m_\sigma(\lambda)$  for three different activation functions, shown in Figure 3, exhibit qualitatively distinct behaviors: absence of a phase transition, a continuous phase transition, and a sharp (discontinuous) phase transition. For  $k_*(\sigma) \geq 3$ , which is the relevant regime for the model (1), the sharp phase transition at  $\lambda_\sigma$  induces a sharp cutoff in the learning of features.

## J Some exact results in the near-interpolation regime

In the near-interpolation regime, certain exact results, such as the leading constants in the asymptotic behavior and the locations of phase transitions, can be computed explicitly as consequences of

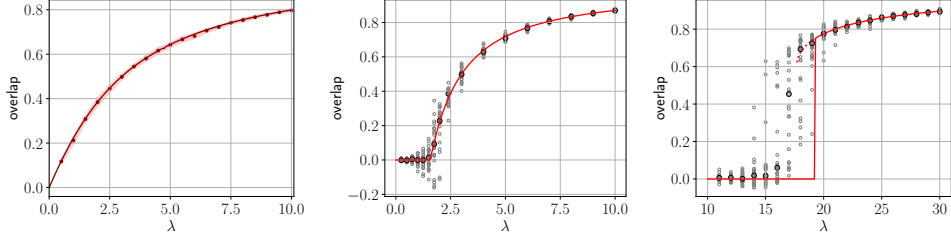


Figure 3: Bayes-optimal overlap as a function of the SNR  $\lambda$  in the generalized linear model in the high-sampling regime of Result 3: comparison between theoretical predictions and HMC simulations initialized on the signal. The experimental data show the overlap between HMC sample and the signal, over 25 independent experiments. The dashed line indicates the metastable solution corresponding to the local maximum near 1 of the function  $\lambda g_\sigma(q) + q + \ln(1 - q)$ , see the discussion concerning metastable solutions in [6]. From left to right: activations  $\text{ReLU}(x)$ ,  $|x|$  and  $\tanh(2x) - cx$ , with  $c = \mathbb{E}_{z \sim \mathcal{N}(0,1)} z \tanh(2z)$ . *Common setting:*  $d = 1000$ ,  $\Delta = 40$ .

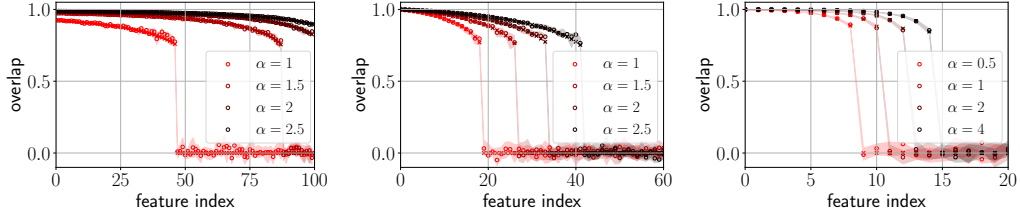


Figure 4: Bayes-optimal feature overlaps in the neural network model (1) for different types of readouts. The crosses show the theoretical prediction, while the circles show experimental results. The circles correspond to the mean overlap computed over 16 independent experiments, and the shaded region indicates the standard deviations. **Left:** dense readout with  $P_v \sim \mathcal{U}([2, 5])/\sqrt{13}$ . **Middle:** power-law readout with  $\beta = 0.7$ . **Right:** exponentially decayed readout, with  $v_j \propto e^{-j/5}$ . *Setting:*  $\sigma(x) = \tanh(2x)$ ,  $d = 200$ ,  $k = 100$ ,  $\Delta = 0.04$ .

Result 1. Although these results are not the primary focus of this paper, they may be of independent interest to some readers. We collect them here.

**Result 6.** Consider the near-interpolation regime with a dense readout  $\mathbf{v}$ , such that the empirical distribution of the entries of  $\sqrt{k}\mathbf{v}$  converges to a limiting distribution  $P_v$  in the infinite-dimensional limit. Define

$$\varepsilon = \lim_{d \rightarrow \infty} \varepsilon^{\text{BO}} \quad (32)$$

$$\mathcal{Q}(\mathbf{v}) = \lim_{\delta \rightarrow 0} \lim_{d \rightarrow \infty} \frac{1}{|I_{\mathbf{v}, \delta}|} \sum_{i \in I_{\mathbf{v}, \delta}} q_i \quad (33)$$

where  $I_{\mathbf{v}, \delta} = \{i \in [k] : \sqrt{k}v_i \in [\mathbf{v} - \delta, \mathbf{v} + \delta]\}$ . Then we have

1.  $(\varepsilon, \mathcal{Q}(\mathbf{v}))$  satisfies the fixed-point equations

$$\mathcal{Q}(\mathbf{v}) = m_\sigma\left(\frac{\alpha \mathbf{v}^2}{\gamma(\Delta + \varepsilon)}\right) \quad (34)$$

$$\varepsilon = g_\sigma(1) - \mathbb{E}_{\mathbf{v} \sim P_v} [\mathbf{v}^2 g_\sigma(\mathcal{Q}(\mathbf{v}))]. \quad (35)$$

2. Let  $\alpha_c(\mathbf{v}) = \sup\{\alpha \geq 0 : \mathcal{Q}(\mathbf{v}) = 0\}$ , then

$$\alpha_c(\mathbf{v}) = \frac{1}{\sqrt{2}} \lambda_\sigma \gamma \left( \Delta + g_\sigma(1) - \mathbb{E}_{\mathbf{v} \sim P_v} \left[ \mathbf{v}^2 g_\sigma \circ m_\sigma \left( \frac{\lambda_\sigma \mathbf{v}^2}{\sqrt{2}} \right) \right] \right).$$

In particular, if  $\max_i v_i$  converges to a limiting value  $v_{\max}$ , then the first phase transition—corresponding to the feature with the largest readout—occurs at

$$\alpha = \frac{\lambda_\sigma \gamma (\Delta + g_\sigma(1))}{v_{\max}^2}. \quad (36)$$

*Proof.* 1. Fix  $i \in I_{v,\delta}$ , we have

$$\frac{(v - \delta)^2}{k} \leq v_i^2 \leq \frac{(v + \delta)^2}{k}$$

Therefore,

$$\frac{n(v - \delta)^2}{kd(\Delta + \varepsilon)} \leq \frac{nv_i^2}{d(\Delta + \varepsilon)} \leq \frac{n(v + \delta)^2}{kd(\Delta + \varepsilon)}$$

Applying the non-decreasing function  $m_\sigma$  on all sides of the previous inequality, we have

$$m_\sigma\left(\frac{n(v - \delta)^2}{kd(\Delta + \varepsilon)}\right) \leq q_i \leq m_\sigma\left(\frac{n(v + \delta)^2}{kd(\Delta + \varepsilon)}\right).$$

The last inequality holds for any  $i \in I_{v,\delta}$ , which implies

$$m_\sigma\left(\frac{n(v - \delta)^2}{kd(\Delta + \varepsilon)}\right) \leq \frac{1}{|I_{v,\delta}|} \sum_{i \in I_{v,\delta}} q_i \leq m_\sigma\left(\frac{n(v + \delta)^2}{kd(\Delta + \varepsilon)}\right).$$

Taking  $d \rightarrow \infty$  in the last inequalities, we obtain

$$m_\sigma\left(\frac{\alpha(v - \delta)^2}{\gamma(\Delta + \varepsilon)}\right) \leq \lim_{d \rightarrow \infty} \frac{1}{|I_{v,\delta}|} \sum_{i \in I_{v,\delta}} q_i \leq m_\sigma\left(\frac{\alpha(v + \delta)^2}{\gamma(\Delta + \varepsilon)}\right).$$

Taking  $\delta \rightarrow 0$ , we have

$$\mathcal{Q}(v) = m_\sigma\left(\frac{\alpha v^2}{\gamma(\Delta + \varepsilon)}\right) \quad (37)$$

$$\varepsilon^{\text{BO}} \sim \sum_{i=1}^k v_i^2 (g_\sigma(1) - g_\sigma(q_i)),$$

taking the limit  $d \rightarrow \infty$ , and using a similar argument in the derivation of (37), we obtain

$$\varepsilon = g_\sigma(1) - \mathbb{E}_{v \sim P_v} [v^2 g_\sigma(\mathcal{Q}(v))] \quad (38)$$

2. From the definition of  $\alpha_c(v)$  and equation (37), using the fact that  $\lambda_\sigma = \sup\{\lambda \geq 0 : m_\sigma(\lambda) = 0\}$ , we have

$$\frac{\alpha_c(v)v^2}{\Delta + \varepsilon} = \lambda_\sigma.$$

Therefore,

$$\begin{aligned} \alpha_c(v) &= \frac{1}{v^2} \lambda_\sigma \gamma (\Delta + \varepsilon) \\ &= \frac{1}{v^2} \lambda_\sigma \gamma (\Delta + g_\sigma(1) - \mathbb{E}_{v \sim P_v} [v^2 g_\sigma \circ \mathcal{Q}(v)]) \\ &= \frac{1}{v^2} \lambda_\sigma \gamma \left( \Delta + g_\sigma(1) - \mathbb{E}_{v \sim P_v} \left[ v^2 g_\sigma \circ m_\sigma \left( \frac{\alpha_c(v)v^2}{\gamma(\Delta + \varepsilon)} \right) \right] \right) \\ &= \frac{1}{v^2} \lambda_\sigma \gamma \left( \Delta + g_\sigma(1) - \mathbb{E}_{v \sim P_v} \left[ v^2 g_\sigma \circ m_\sigma \left( \frac{\lambda_\sigma v^2}{v^2} \right) \right] \right) \end{aligned}$$

If  $v = v_{\max}$ , then for any  $v \in \text{supp}(P_v)$ , we have  $\lambda_\sigma v^2 / v^2 \leq \lambda_\sigma$ , so  $m_\sigma(\lambda_\sigma v^2 / v^2) = 0$ . The formula simplifies to

$$\alpha_c(v_{\max}) = \frac{\lambda_\sigma \gamma (\Delta + g_\sigma(1))}{v_{\max}^2}.$$

□

**Result 7.** Consider the near-interpolation regime with power-law readouts with exponent  $\beta$ , i.e.

$$v_i^2 = \frac{i^{-2\beta}}{\sum_{j=1}^k j^{-2\beta}}, \quad i \in [k].$$

1. If  $k_c < k$  and  $i = \lfloor xk_c \rfloor$  for some  $x \in (0, 1)$ , then

$$\lim_{d \rightarrow \infty} q_i = m_\sigma(\lambda_\sigma x^{-2\beta}) := \phi(x) \quad (39)$$

In other words, the overlaps  $(q_i)_{i=1}^k$  in the infinite dimension limit can be compactly described by a limiting profile  $\phi$ .

2. For  $\beta > 1/2$ , let

$$\bar{k}_c = \lim_{d \rightarrow \infty} k_c d^{-\frac{1}{2\beta}}, \quad \varepsilon^{\text{BO}} = \lim_{d \rightarrow \infty} \varepsilon^{\text{BO}} d^{-\frac{1}{2\beta}+1}, \quad (40)$$

Then, letting  $z(\beta) := \sum_{i=1}^{\infty} i^{-2\beta}$  and since  $\varepsilon = 0$ ,

$$\bar{k}_c = \left( \frac{\alpha}{\lambda_\sigma z(\beta) \Delta} \right)^{\frac{1}{2\beta}} \quad (41)$$

$$\varepsilon^{\text{BO}} = \frac{\bar{k}_c^{1-2\beta}}{z(\beta)} \left( \int_0^1 \frac{g_\sigma(1) - g_\sigma(\phi(x))}{x^{2\beta}} dx + \frac{g_\sigma(1)}{(2\beta - 1)} \right). \quad (42)$$

3. For  $\beta < 1/2$ , let

$$\bar{k}_c = \lim_{d \rightarrow \infty} k_c/k, \quad \varepsilon = \lim_{d \rightarrow \infty} \varepsilon^{\text{BO}}. \quad (43)$$

Then  $\varepsilon$  is the unique solution in  $(0, \infty)$  of

$$\frac{g_\sigma(1) - \varepsilon}{1 - 2\beta} = \int_0^1 x^{-2\beta} g_\sigma \circ m_\sigma \left( \frac{\alpha(1 - 2\beta)}{\gamma(\Delta + \varepsilon)} x^{-2\beta} \right) dx \quad (44)$$

and

$$\bar{k}_c = \left( \frac{(1 - 2\beta)\alpha}{\lambda_\sigma \gamma(\Delta + \varepsilon)} \right)^{\frac{1}{2\beta}} \quad (45)$$

Moreover, in the thermodynamic limit, all features are learnable if and only if  $\alpha > \alpha_*$ , where

$$\frac{\alpha_*}{\lambda_\sigma \gamma} = \frac{\Delta + g_\sigma(1)}{1 - 2\beta} - \int_0^1 \frac{g_\sigma(\phi(x))}{x^{2\beta}} dx, \quad (46)$$

*Derivation.* 1. We have

$$\frac{nv_{k_c+1}^2}{d(\Delta + \varepsilon^{\text{BO}})} < \lambda_\sigma < \frac{nv_{k_c}^2}{d(\Delta + \varepsilon^{\text{BO}})}. \quad (47)$$

From the inequality on the left, it is clear that  $k_c \rightarrow \infty$  as  $d \rightarrow \infty$ . This implies  $\lim_{d \rightarrow \infty} v_{k_c}/v_{k_c+1} = 1$ , which yields

$$\lim_{d \rightarrow \infty} \frac{nv_{k_c}^2}{d(\Delta + \varepsilon^{\text{BO}})} = \lambda_\sigma. \quad (48)$$

Next, let  $x \in (0, 1)$  and  $i = \lfloor xk_c \rfloor$ . Recall that

$$q_i \simeq m_\sigma \left( \frac{nv_i^2}{d(\Delta + \varepsilon^{\text{BO}})} \right) \quad (49)$$

Sending  $d \rightarrow \infty$  on both sides of (49), and using the fact that

$$\lim_{d \rightarrow \infty} \frac{nv_i^2}{d(\Delta + \varepsilon^{\text{BO}})} = \lim_{d \rightarrow \infty} \frac{nv_{k_c}^2}{d(\Delta + \varepsilon^{\text{BO}})} \frac{v_i^2}{v_{k_c}^2} = \lambda_\sigma x^{-2\beta}, \quad (50)$$

we obtain

$$\lim_{d \rightarrow \infty} q_i = m_\sigma(\lambda_\sigma x^{-2\beta}) = \phi(x) \quad (51)$$

2. From (48), straightforward calculations yield

$$\lim_{d \rightarrow \infty} k_c d^{-\frac{1}{2\beta}} = \left( \frac{\alpha}{\lambda_\sigma z(\beta)(\Delta + \varepsilon)} \right)^{\frac{1}{2\beta}}. \quad (52)$$

Next, using  $q_i \simeq \phi(i/k_c)$  for  $i \leq k_c$ , the error contributed by learnable features is

$$\begin{aligned} & \sum_{i \leq k_c} \frac{i^{-2\beta}}{z(\beta)} (g_\sigma(1) - g_\sigma \circ \phi(i/k_c)) \\ &= k_c^{1-2\beta} \frac{1}{k_c} \sum_{i \leq k_c} \frac{(i/k_c)^{-2\beta}}{z(\beta)} (g_\sigma(1) - g_\sigma \circ \phi(i/k_c)) \end{aligned} \quad (53)$$

$$\simeq k_c^{1-2\beta} \int_0^1 \frac{x^{-2\beta}}{z(\beta)} (g_\sigma(1) - g_\sigma(\phi(x))) dx. \quad (54)$$

where in the last step, averaged sum over  $i \leq k_c$  is asymptotically the integral over  $[0, 1]$ .

On the other hand, since  $q_i = 0$  as  $i > k_c$ , the error that comes from non-learnable features is

$$\sum_{i > k_c} v_i^2 g_\sigma(1) \simeq g_\sigma(1) \sum_{i > k_c} \frac{i^{-2\beta}}{z(\beta)} \simeq \frac{g_\sigma(1)}{(2\beta - 1)z(\beta)} k_c^{1-2\beta} \quad (55)$$

This implies  $\varepsilon^{\text{BO}} \propto d^{\frac{1}{2\beta}-1}$ , so  $\varepsilon = \lim_{d \rightarrow \infty} \varepsilon^{\text{BO}} = 0$ . Plug this value of  $\varepsilon$  to the previous formula, we obtain the results for  $\beta > 1/2$ .

3. We have

$$v_i^2 = \frac{i^{-2\beta}}{\sum_{j=1}^k j^{-2\beta}} \simeq (1 - 2\beta) i^{-2\beta} k^{2\beta-1} \quad (56)$$

From (48), straightforward calculations yield

$$\lim_{d \rightarrow \infty} k_c/k = \left( \frac{(1 - 2\beta)\alpha}{\lambda_\sigma \gamma (\Delta + \varepsilon)} \right)^{\frac{1}{2\beta}} \quad (57)$$

In this case it is possible for all features to be learnable. Let us denote

$$\alpha_\star = \lim_{d \rightarrow \infty} \alpha_c(k) \quad (58)$$

where we recall that  $\alpha_c(k)$  is the threshold of  $\alpha$  for the feature  $k$  to be learnable. Let  $\varepsilon$  be the BO error at this value of  $\alpha$ . We have

$$\begin{aligned} \alpha_c(k) &\simeq \frac{\lambda_\sigma (\Delta + \varepsilon)}{dv_k^2} \\ &= \frac{\lambda_\sigma}{dv_k^2} \left( \Delta + g_\sigma(1) - \sum_{i=1}^k v_i^2 g_\sigma(q_i) \right) \\ &= \frac{\lambda_\sigma}{dv_k^2} \left( \Delta + g_\sigma(1) - \sum_{i=1}^k v_i^2 g_\sigma \circ m_\sigma \left( \frac{\alpha_c(k) dv_i^2}{\Delta + \varepsilon} \right) \right) \\ &= \frac{\lambda_\sigma}{dv_k^2} \left( \Delta + g_\sigma(1) - \sum_{i=1}^k v_i^2 g_\sigma \circ m_\sigma \left( \lambda_\sigma \frac{v_i^2}{v_k^2} \right) \right) \end{aligned}$$

Using the fact that  $v_k^2 \sim (1 - 2\beta)/k$ ,  $v_i^2/v_k^2 = (i/k)^{-2\beta}$  and  $v_i^2 \sim (1 - 2\beta)i^{-2\beta}k^{2\beta-1}$ , the last expression can be written as a Riemann sum, which in the limit  $d \rightarrow \infty$  gives

$$\alpha_\star = \frac{\lambda_\sigma \gamma (\Delta + g_\sigma(1))}{1 - 2\beta} - \lambda_\sigma \gamma \int_0^1 \frac{g_\sigma(\phi(x))}{x^{2\beta}} dx, \quad (59)$$

Let us derive the fixed-point equation for  $\varepsilon$ . We have

$$\begin{aligned}
\varepsilon &= g_\sigma(1) - \sum_{i=1}^k v_i^2 g_\sigma(q_i) \\
&\sim g_\sigma(1) - (1-2\beta)k^{2\beta-1} \sum_{i=1}^k i^{-2\beta} g_\sigma \circ m_\sigma \left( \frac{\alpha d v_i^2}{\Delta + \varepsilon} \right) \\
&\sim g_\sigma(1) - (1-2\beta)k^{2\beta-1} \sum_{i=1}^k i^{-2\beta} g_\sigma \circ m_\sigma \left( \frac{\alpha(1-2\beta)}{\gamma(\Delta + \varepsilon)} (i/k)^{-2\beta} \right) \\
&\sim g_\sigma(1) - (1-2\beta) \frac{1}{k} \sum_{i=1}^k (i/k)^{-2\beta} g_\sigma \circ m_\sigma \left( \frac{\alpha(1-2\beta)}{\gamma(\Delta + \varepsilon)} (i/k)^{-2\beta} \right) \\
&\sim g_\sigma(1) - (1-2\beta) \int_0^1 x^{-2\beta} g_\sigma \circ m_\sigma \left( \frac{\alpha(1-2\beta)}{\gamma(\Delta + \varepsilon)} x^{-2\beta} \right) dx
\end{aligned}$$

which gives the fixed point equation for  $\varepsilon$ .

*Remark 8.* The following properties of the limiting profile  $\phi(x) = m_\sigma(\lambda_\sigma x^{-2\beta})$  can be derived from properties of  $m_\sigma$  in Appendix D.

1.  $\phi(x)$  is non-increasing
2.  $\lim_{x \rightarrow 0} \phi(x) = 1, \lim_{x \rightarrow 1} \phi(x) = q_\sigma$ .
3.  $\phi(x) = 1 - cx^{2\beta} + o(x^{2\beta})$  as  $x \rightarrow 0^+$ , for some  $c > 0$

## K Numerical methods

### K.1 Solving the fixed point equations

From the system of fixed point equations, we obtain the following equation for  $\varepsilon$ :

$$\varepsilon = g_\sigma(1) - \sum_{i=1}^k v_i^2 g_\sigma \circ m_\sigma \left( \frac{nv_i^2/d}{\Delta + \varepsilon} \right). \quad (60)$$

This can be quickly solved by a standard numerical method such as bisection.

### K.2 HMC simulation

The theoretical predictions for the overlaps are validated by HMC simulation. In general, sampling from the posterior is difficult since the posterior landscape can be extremely complicated: with random initialization, it can take exponentially long to reach the true equilibrium. However, if the initialization lies in the same basin of attraction as the equilibrium state, convergence is achieved with reasonable computational cost. We initialize such that the first  $k_c$  rows coincide with the ground truth, and the remaining rows are random. Note that the HMC does not validate the prediction of  $k_c$  itself.

### K.3 Numerical evaluation of Bayes-optimal error

Directly evaluating the Bayes-optimal error from its definition is computationally expensive. Indeed, computing  $\mathbb{E}[y(\mathbf{x}, \mathbf{W} \mid \mathcal{D})]$  requires drawing many independent samples from the posterior distribution  $P(\mathbf{W} \mid \mathcal{D})$ , and each sample requires a computational time on the order of  $10^2$  seconds on a GPU. To overcome this difficulty, we compute the Bayes-optimal error through *Gibbs error*, defined as

$$\varepsilon^{\text{Gibbs}} = \mathbb{E}_{\mathcal{D}, \mathbf{W}^0, \mathbf{W}^1} \mathbb{E}_{\mathbf{x} \sim \mathcal{N}(0, \mathbf{I}_d)} (y(\mathbf{x}, \mathbf{W}^0) - y(\mathbf{x}, \mathbf{W}^1))^2, \quad (61)$$

where  $\mathbf{W}^1$  is a sample of  $P(\mathbf{W} \mid \mathcal{D})$ . It is known that  $\varepsilon^{\text{BO}} = \frac{1}{2} \varepsilon^{\text{Gibbs}}$ . This identity is a straightforward generalization of the identity  $\mathbb{E}(X - X')^2 = 2\mathbb{E}(X - \mathbb{E}X)^2$  for any i.i.d. random variables

$X, X'$ . In practice, one only needs  $10\text{-}10^2$  samples of  $(\mathcal{D}, \mathbf{W}^0, \mathbf{W}^1)$  due to small fluctuations with respect to these variables, while averaging over  $\mathbf{x}$  requires  $10^4\text{-}10^5$  samples, each of which can be generated at small cost. Computing the optimal error via Gibbs error is much more efficient, as for each fixed  $(\mathcal{D}, \mathbf{W}^0)$ , only one posterior sample from  $P(\mathbf{W} \mid \mathcal{D})$  is needed.

#### **K.4 Training with SGD**

We use the ADAM optimizer implemented in Pytorch to train the student network. We note here some important points in the training

1. The student's features are normalized after each epoch, preventing their norms from growing excessively and resulting in more stable and well-behaved training dynamics.
2. Performance degrades when the student's readout is fixed to match the teacher during training, as the student is more likely to get stuck in local minima. In contrast, when the student readout is learnable, it still recovers that of the teacher, and the possibility for the readout to change during training helps the student escape local minima.